Mechanical Systems and Signal Processing 24 (2010) 1977–1997

Contents lists available at ScienceDirect

Mechanical Systems and Signal Processing

journal homepage: www.elsevier.com/locate/jnlabr/ymssp

Vibration based health monitoring for a lightweight truss structure: Experimental assessment of several statistical time series methods

F.P. Kopsaftopoulos, S.D. Fassois *

Stochastic Mechanical Systems and Automation (SMSA) Laboratory, Department of Mechanical and Aeronautical Engineering, University of Patras, GR 265 00, Greece

ARTICLE INFO

Article history:
Received 14 May 2010
Accepted 17 May 2010
Available online 25 May 2010

Keywords:
Structural health monitoring
Statistical time series methods
Damage detection
Damage identification
Vibration based methods
Structural identification

ABSTRACT

An experimental assessment of several vibration based statistical time series methods for structural health monitoring (SHM) is presented via their application to a lightweight aluminum truss structure. A concise overview of the main non-parametric and parametric methods is provided, including response-only and excitation–response schemes. Damage detection and identification is based on univariate (scalar) versions of the methods, while results for three distinct vibration measurement positions on the structure are presented. The methods' effectiveness is assessed via multiple experiments under various damage scenarios. The results of the study confirm the high potential and effectiveness of statistical time series methods for SHM.

1. Introduction

Vibration based structural damage detection, identification (localization) and magnitude estimation, also collectively referred to as damage diagnosis, is of paramount importance for reasons associated with proper operation, maintenance and safety. The process of implementing a damage diagnosis strategy is referred to as structural health monitoring (SHM). This process involves the observation of a structure/system over time using periodical measurements, the extraction of damage sensitive quantities (features) from these measurements, and the statistical analysis of these quantities in order to determine the current structural state.

Over the past several years, a wide variety of local non-destructive testing tools have been developed [1–3]. These are mainly based on ultrasound, acoustic, radiography, eddy current, and thermal field principles, and require access to the vicinity of the suspected damage location, while they are typically time consuming and costly. Aiming at overcoming the aforementioned drawbacks, SHM methods attempt to achieve damage diagnosis on a more "global" basis, with no requirement for visual inspection and potential automation capability. Among them, vibration based methods [1–4] appear promising, as they tend to be time effective and less expensive than many alternatives.

Statistical time series methods for SHM form an important, rapidly evolving, category within the broader vibration based family of methods [5–11]. They utilize (i) random excitation and/or response signals (time series), (ii) statistical model building, and (iii) statistical decision making for inferring the health state of a structure. As with all vibration based methods, the fundamental principle upon which they are founded is that small changes (damage) in a structure cause discrepancies in its vibration response, which may be detected and associated with a specific cause (damage type).

* Corresponding author.
E-mail addresses: fkopsaf@mech.upatras.gr (F.P. Kopsaftopoulos), fassois@mech.upatras.gr (S.D. Fassois).

0888-3270/$ - see front matter
doi:10.1016/j.ymssp.2010.05.013

Statistical time series methods for SHM are fundamentally of the inverse type, as the models used are *data based* rather than physics based. Furthermore, they offer a number of important advantages, including inherent accounting for uncertainties, no need to interrupt normal operation, no requirement for physics-based or finite element (FE) type models, no requirement for complete modal models, and statistical decision making with specified performance characteristics. On the other hand, as complete structural models are not employed, time series methods may identify damage only to the extent allowed by the type of model used. Other limitations include the need for proper "training", adequate user expertise and potentially limited physical insight. For an extended overview of the principles and techniques of statistical time series methods for SHM, the interested reader is referred to the recent overviews by the second author and co-workers [5,6].

Statistical time series methods for SHM use scalar or vector random signals from the structure in its healthy state, as well as from a number of potential damage states, identifying suitable (parametric or non-parametric) statistical time series models describing the structure in each state, and extracting a statistical quantity (characteristic quantity) characterizing the structural state in each case (baseline phase). Damage diagnosis is then accomplished via statistical decision making consisting of comparing, in a statistical sense, the current characteristic quantity with that of each potential state as determined in the baseline phase (inspection phase).

Non-parametric time series methods for SHM are those based on corresponding time series representations, such as power spectral estimates [5,6]. This type of methods has received limited attention in the literature. Sakellariou et al. [12] present the application of a power spectral density (PSD) based method to fault detection in a railway vehicle suspension. The method is applied within a statistical framework, utilizing interval spectral estimates and statistical decision making schemes, while its effectiveness is assessed via experimental data. Furthermore, the application of a PSD analysis based method to a simply supported aluminum beam is presented by Liberatore and Carman [13], although the effectiveness of the method is demonstrated in conjunction with an analytical model, without employing statistical tools. Rizos et al. [14] treat the problem of damage detection in stiffened aircraft panels via a non-parametric frequency response function (FRF) based method. The FRF estimates are demonstrated to exceed their normal variability bounds under skin damage, while the method accounts for uncertainties and statistical variabilities. Finally, Hwang and Kim [15] present an FRF based method, whose effectiveness is numerically demonstrated via simulation examples based on finite element models of a simple cantilever and a helicopter rotor blade. Although no statistical framework is incorporated, the method is reported to achieve a satisfactory level of precision with respect to damage diagnosis.

Parametric time series methods for SHM are those based on corresponding time series representations, such as the AutoRegressive Moving Average (ARMA) representation [5,6,16]. This type of methods has attracted considerable attention and their principles have been used in a number of studies. Sohn et al. [17,18] use the prediction errors of a so-called AutoRegressive and AutoRegressive with eXogenous inputs (AR-ARX) model, a sequential hypothesis testing technique (sequential probability ratio test), and extreme value statistics for damage diagnosis. The method is assessed via numerical simulations and its application to an eight degree-of-freedom mass–spring system, data obtained from a patrol boat, and a three-storey building model. In a related work, Sohn and Farrar [19] employ the standard deviation ratio of the residual errors from a two-stage AR-ARX model, obtained from healthy measured signals, as the damage sensitive feature. Under the normality assumption this feature is shown to follow *F* distribution based on which a hypothesis test is developed to infer the structural health state of an eight degree-of-freedom mass–spring system. Adams and Farrar [20] discuss the use of the autoregressive and exogenous coefficients of a frequency domain ARX model and their implementation for damage diagnosis. The model coefficients are utilized for detecting damage with some level of statistical confidence by applying a standard statistical measure (Mahalanobis distance), while the proposed method is applied to data obtained from a three-storey building model.

Furthermore, the first three autoregressive coefficients of an ARMA model constitute the feature vector employed by Nair et al. [21,22] to tackle damage detection. A Gaussian mixture model is used to model the feature vector, while damage is detected via the gap statistic. The postulated method is applied to analytical and experimental data from the ASCE benchmark structure. Carden and Brownjohn [23] propose a damage detection method based on the ARMA model residual sum of squares and a statistical classifier utilizing a χ^2 distribution. The experimental assessment of the method is achieved via its application to the IASC-ASCE four-storey frame structure, the Z24 bridge, and the Malaysia–Singapore Second Link bridge. Fugate et al. [24] fit an AR model to the measured data obtained from a healthy structure and the corresponding model residuals are used as damage sensitive features. Next, statistical process control methods, such as the X-bar and S control charts, are employed to monitor the mean and variance of the selected features in order to detect damage. For demonstration, the method is applied to vibration test data acquired from a concrete bridge column. An estimate of the standard deviation along with higher-order moments of the residuals obtained from vector AR models is used to detect damage by Mattson and Pandit [25]. A damage detection threshold level is identified from available training data, while the method is assessed via data obtained from an eight degree-of-freedom test bed. Gao and Lu [26] present a formulation that enables the construction of residual generators, via state-space representations, as damage indicators. Then, damage detection is transformed into a disturbance decoupling problem, so that a geometric technique can be employed to detect damage. Numerical results and experimental examples on a laboratory test frame are used to assess the effectiveness of the method. A two-stage damage diagnosis strategy is proposed by Zheng and Mita [27]. Damage existence is determined in the first stage using a damage indicator defined as the distance between two ARMA models, while, in a second stage, damage localization is achieved via pre-whitening filters. The method does not incorporate a statistical framework, while it is applied to a five-storey steel structure. Sakellariou and Fassois [28] employ output error

(OE) models and statistical hypothesis testing procedures utilizing the corresponding model parameter vectors, in order to achieve damage diagnosis in structures under earthquake excitation. Damage identification (localization) is achieved via a geometric method, where the parameter vector is used as an initial feature vector, while the method's effectiveness is assessed via a six-storey building model.

A method based on subspace identification and state space model residuals is reported in [7,8], while methods based on the novel class of stochastic functionally pooled (FP) models are reported in [9,10]. The FP model based methods are capable of offering an effective solution to the damage detection, localization and magnitude (size) estimation subproblems within a unified framework. Nevertheless, these methods are somewhat more elaborate.

In spite of the progress achieved so far, the literature on vibration based statistical time series methods for SHM remains relatively sparse. In particular, no application studies that experimentally compare and assess the various methods are available. The *goal* of the present study precisely is the experimental comparison and assessment of a number of *univariate* (scalar) statistical time series methods to a lightweight laboratory aluminum truss structure. The damage cases considered correspond to loosening of various bolts connecting certain of the truss elements. Random force excitation is provided via an electromechanical shaker, while the vibration responses are measured at various positions via dynamic strain gauges. Two non-parametric methods, namely a power spectral density (PSD) and a frequency response function (FRF) based method, as well as four parametric methods, namely a model parameter based, a residual variance, a residual likelihood function, and a residual uncorrelatedness based method, are briefly reviewed and experimentally assessed.

As already indicated, *univariate* (scalar response) versions of the methods are used, while results are presented for *three* distinct vibration response positions designated as Y1, Y2 and Y3. The methods' main features and operational characteristics are discussed along with practical issues, while their effectiveness is demonstrated via various test cases corresponding to different experiments, damage scenarios, and vibration measurement positions.

The rest of the paper is organized as follows: The experimental set-up is presented in Section 2, while the general workframe of statistical time series methods for SHM is briefly outlined in Section 3. A concise overview of the methods is given in Section 4, and the experimental assessment and comparison are presented in Section 5. Concluding remarks are finally summarized in Section 6.

2. The experimental set-up

2.1. The structure

The truss structure is depicted in Fig. 1, suspended through a set of cords. It consists of 28 elements with rectangular cross sections (15×15 mm) jointed together via steel elbow plates and bolts. All parts are constructed from standard aluminum with the overall dimensions being $1400 \times 700 \times 800 \times 700$ mm.

2.2. The damage types and the experiments

The damages considered correspond to complete loosening of various bolts at different joints of the structure. Five distinct types are specifically considered (Fig. 1): The first damage type, referred to as *damage type A*, corresponds to the loosening of bolt A1 joining together a horizontal with a vertical element. The second damage type, referred to as *damage type B*, corresponds to the loosening of bolts A1 and B1 joining together a horizontal with a vertical element. Damage type B affects the same elements as damage type A, but it is more severe, as loosening of two bolts is involved. The third damage type, referred to as *damage type C*, corresponds to the loosening of bolts C1 and C2 joining together a horizontal with a

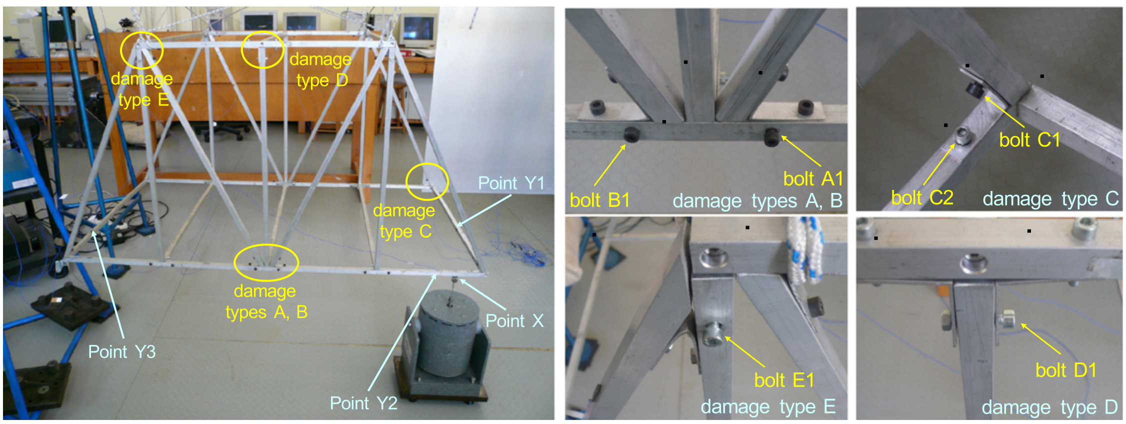

Fig. 1. The aluminum truss structure and the experimental set-up: the force excitation (Point X), the vibration measurement positions (Points Y1–Y3), and the considered damage types (A, B, C, D, and E).

Table 1
The considered damage types, number of experiments, and vibration signal details.

Structural state	Description	Total number of experiments
Healthy	–	40 (1 baseline)
Damage type A	Loosening of bolt A1	32 (1 baseline)
Damage type B	Loosening of bolts A1 and B1	32 (1 baseline)
Damage type C	Loosening of bolts C1 and C2	32 (1 baseline)
Damage type D	Loosening of bolt D1	32 (1 baseline)
Damage type E	Loosening of bolt E1	32 (1 baseline)

Sampling frequency: f_s=256 Hz, signal bandwidth: $[0.5-100]$ Hz.
Signal length N in samples (s): non-parametric methods: N=30 720 (120 s), parametric methods: N=10 000 (39 s).

diagonal element. The fourth damage type, referred to as *damage type D*, corresponds to the loosening of bolt D1 joining together a horizontal with a vertical element. Finally, the fifth damage type, referred to as *damage type E*, corresponds to the loosening of bolt E1 joining together a vertical with a diagonal element. All damage types considered are summarized in Table 1.

The force excitation is a random Gaussian signal applied vertically at Point X (Fig. 1) via an electromechanical shaker (MB Dynamics Modal 50A, max load 225 N) equipped with a stinger, and measured via an impedance head (PCB 288D01, sensitivity 98.41 mV/lb). The vibration responses are measured at different points via dynamic strain gauges (PCB ICP 740B02, 0.005–100 kHz, 50 mV/$\mu\varepsilon$; sampling frequency f_s=256 Hz, signal bandwidth 0.5–100 Hz). The force and strain signals are driven through a signal conditioning device (PCB 481A02) into the data acquisition system (SigLab 20–42). In this study damage detection and identification results based on each one of the three vibration response signals (Points Y1, Y2 and Y3—Fig. 1) and obtained via *scalar* versions of the methods are presented. This allows examination of the potential of the methods to achieve damage detection and identification even through a single vibration signal measurement.

A significant number of test cases is considered in the experimental assessment: In each test case a specific experiment (out of a total of 40 experiments for the healthy structure and 32 experiments for each damage state, with one from each category reserved for the baseline phase—Table 1) and vibration response measurement position (Points Y1–Y3, Fig. 1) are employed. Experimental details are presented in Table 1. Notice that the sample mean is subtracted from each signal and scaling by the signal's sample standard deviation is implemented.

3. Workframe of statistical time series methods for SHM

Let S_o designate the structure under consideration in its *nominal* (healthy) state, $S_A, S_B, \ldots$ the structure under damage of *type* (*mode*) $A, B, \ldots$ and so on, and S_u the structure in unknown (to be determined) state. Each damage type may include a continuum of damages which are characterized by common nature or location (for instance, damage in a specific structural element) but varying degree of damage.

Statistical time series methods are commonly based on discretized excitation $x[t]$ and/or response $y[t]$ (for $t=1, 2, \ldots, N$) random vibration data records. Note that t refers to discrete time, with the corresponding actual time being $(t-1)T_s$, where T_s stands for the sampling period. Let the complete excitation and response signals be presented as X and Y, that is $Z=(X, Y)$. Like before, a subscript $(o, A, B, \ldots, u)$ is used for designating the corresponding state of the structure that provided the signals.

Note that all collected signals need to be suitably pre-processed [3,5,29]. This may include low or band-pass filtering within the frequency range of interest, signal subsampling (in case the originally used sampling frequency is too high), sample mean subtraction, as well as proper scaling (in the linear dynamics case). The latter is not only used for numerical reasons, but also for counteracting—to the extent possible—different operating (including excitation levels) and/or environmental conditions.

The obtained signals are subsequently analyzed by parametric or non-parametric time series methods and appropriate models are identified and properly validated [5,6,16]. Such models are identified on the basis of data $Z_o, Z_A, Z_B, \ldots$ in the *baseline phase* and based on Z_u in each *inspection phase*. From each estimated model, the corresponding estimate of a *characteristic quantity* Q is extracted ($\widehat{Q}_o$, $\widehat{Q}_A$, $\widehat{Q}_B$, ... in the baseline phase; $\widehat{Q}_u$ in the inspection phase—see Table 2).

Damage detection is then based on proper comparison of the true (but not precisely known) Q_u to the true (but also not precisely known) Q_o via a binary statistical hypothesis test that uses the corresponding estimates—see Table 3. *Damage identification* is similarly based on the proper comparison Q_u to each one of $Q_A, Q_B, \ldots$ via statistical hypothesis testing procedures that also use the corresponding estimates (Table 3). *Damage magnitude estimation*, when considered, is based on interval estimation techniques. The general workframe for statistical time series methods for SHM is depicted in Fig. 2.

Note that the design of a binary statistical hypothesis test is generally based on the probabilities of *type I* and *type II* error, or else the *false alarm* (α) and *missed damage* (β) probabilities. The designs presented in this work are based on the former, but in selecting α it should be born in mind that as α decreases (increases) β increases (decreases).

Table 2
Workframe set-up: structural state, vibration signals used, and the characteristic quantity (baseline and inspection phases).

Baseline phase				
Structural state	S_o (healthy structure)	S_A (damage type A)[a]	S_B (damage type B)[a]	…
Vibration signals	$z_o[t]=(x_o[t], y_o[t])$	$z_A[t]=(x_A[t], y_A[t])$	$z_B[t]=(x_B[t], y_B[t])$	…
	$Z_o=(X_o,Y_o)$	$Z_A=(X_A,Y_A)$	$Z_B=(X_B,Y_B)$	…
Characteristic quantity	Q_o	Q_A	Q_B	…
Inspection phase				
Structural state	S_u (current structure in unknown state)			
Vibration signals	$z_u[t]=(x_u[t], y_u[t])$			
	$Z_u=(X_u,Y_u)$			
Characteristic quantity	Q_u			

[a] Normally various damage magnitudes are considered.

Table 3
Statistical hypothesis testing problems for the damage detection and identification tasks.

Damage detection	
$H_0 : Q_u \sim Q_o$	Null hypothesis — healthy structure
$H_1 : Q_u \nsim Q_o$	Alternative hypothesis — damaged structure
Damage identification	
$H_A : Q_u \sim Q_A$	Hypothesis *A* — damage type A
$H_B : Q_u \sim Q_B$	Hypothesis *B* — damage type B
$\vdots$	$\vdots$

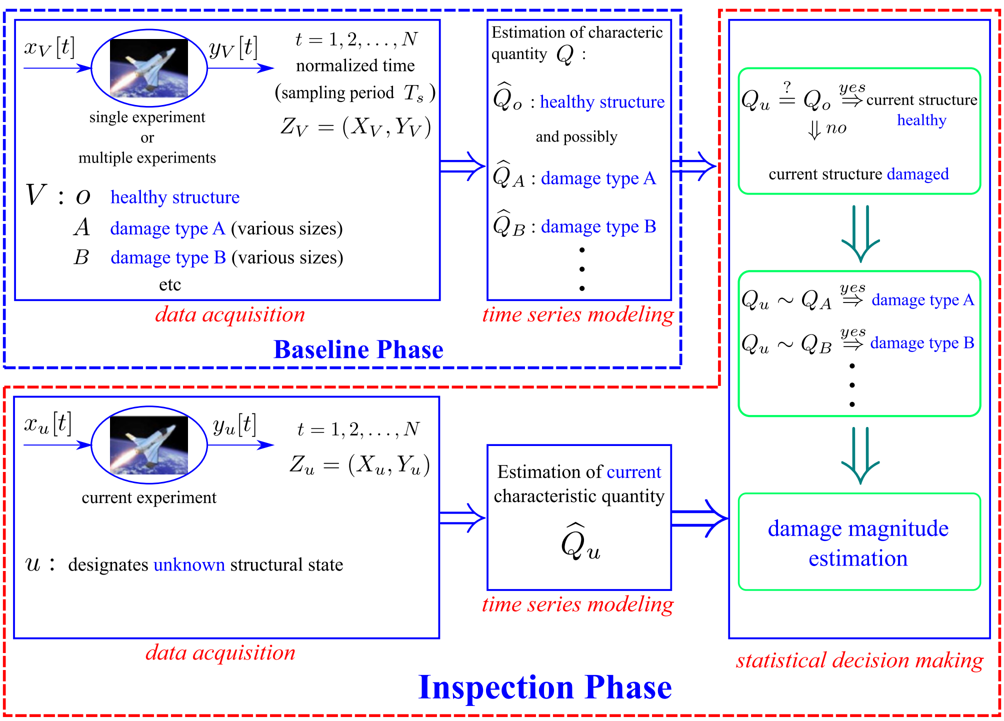

Fig. 2. Workframe for statistical time series methods for structural health monitoring.

4. Concise overview of selected statistical time series methods for SHM

A concise overview of selected statistical time series methods for SHM is presented—for further details the reader is referred to [5,6]. Statistical time series methods may be classified as *non-parametric* or *parametric*, depending on the way the characteristic quantity Q is constructed [5,6]. Non-parametric methods utilize a statistic based on non-parametric time series representations, such as spectral models [5,6]. On the other hand, parametric methods utilize a statistic Q based on parametric time series representations, such as AutoRegressive with eXogenous excitation (ARX) or other representations [16,29]. Depending on whether the response only or the excitation and the response signals are employed, the methods are also classified as *response-only* or *excitation–response*, respectively.

4.1. Non-parametric methods

4.1.1. A power spectral density (PSD) based method

Damage detection and identification is tackled via changes in the power spectral density (PSD) of the measured vibration response signals when the excitation is not available (*response-only* case). The method's characteristic quantity thus is $Q=S_{yy}(\omega)=S(\omega)$, with ω designating frequency. The main idea is based on the comparison of the current (*unknown*) structural response's PSD $S_u(\omega)$ to that of the healthy structure's $S_o(\omega)$—or, in fact, to that corresponding to any other structural condition. The following hypothesis testing problem is then set up for damage detection:

$$\begin{aligned} &H_0 : S_u(\omega)=S_o(\omega) \quad \text{(null hypothesis — healthy structure)}\\ &H_1 : S_u(\omega)\neq S_o(\omega) \quad \text{(alternative hypothesis — damaged structure).}\end{aligned} \tag{1}$$

As the true PSDs, $S_u(\omega)$, $S_o(\omega)$, are unknown, their estimates $\widehat{S}_u(\omega)$, $\widehat{S}_o(\omega)$ obtained via the Welch method (with K non-overlapping segments; refer to Table 4) are used [30, pp. 3 and 76]. Then, the following quantity follows (for each frequency ω) F distribution with $(2K, 2K)$ degrees of freedom [5,6]:

$$F=\frac{\widehat{S}_o(\omega)/S_o(\omega)}{\widehat{S}_u(\omega)/S_u(\omega)} \sim F(2K,2K). \tag{2}$$

Under the null (H_0) hypothesis the true PSDs coincide ($S_u(\omega)=S_o(\omega)$) and $F=\widehat{S}_o(\omega)/\widehat{S}_u(\omega)$. This should then be in the range $[f_{\alpha/2}, f_{1-\alpha/2}]$ with probability $1-\alpha$, and decision making is as follows at a selected α risk level (type I error probability of α):

$$\begin{aligned} &f_{\alpha/2}(2K,\,2K)\leq F\leq f_{1-\alpha/2}(2K,\,2K) \quad (\forall\,\omega)\Longrightarrow H_0 \text{ is accepted} \quad \text{(healthy structure)}\\ &\text{Else} \Longrightarrow H_1 \text{ is accepted} \quad \text{(damaged structure),}\end{aligned} \tag{3}$$

with $f_{\alpha/2}, f_{1-\alpha/2}$ designating the F distribution's $\alpha/2$ and $1-\alpha/2$ critical points.

Note that damage identification may be similarly achieved by performing hypotheses testing similar to the above for damages from each potential damage type (see Table 3).

4.1.2. A frequency response function (FRF) based method

This method is similar, but requires the availability of both the excitation and response signals (*excitation–response* case) and uses the FRF magnitude as its characteristic quantity $Q=|H(j\omega)|$. The main idea is the comparison of the FRF magnitude $|H_u(j\omega)|$ of the current state of the structure to that of the healthy structure $|H_0(j\omega)|$. The following hypothesis testing problem is then set up for damage detection:

$$\begin{aligned} &H_0 : \delta|H(j\omega)|=|H_0(j\omega)|-|H_u(j\omega)|=0 \quad \text{(null hypothesis — healthy structure)}\\ &H_1 : \delta|H(j\omega)|=|H_0(j\omega)|-|H_u(j\omega)|\neq 0 \quad \text{(alternative hypothesis — damaged structure).}\end{aligned} \tag{4}$$

As the true FRFs, $H_u(j\omega)$ and $H_0(j\omega)$, are unknown, their respective estimates, $\widehat{H}_u(j\omega)$ and $\widehat{H}_0(j\omega)$, obtained as indicated in Table 4, are used. The FRF estimator may, asymptotically ($N\to\infty$), be considered as approximately following Gaussian distribution [31, p. 338]. Under the null (H_0) hypothesis the true FRF magnitudes coincide ($|H_u(j\omega)|=|H_0(j\omega)|$), hence $\delta|\widehat{H}(j\omega)|=|\widehat{H}_0(j\omega)|-|\widehat{H}_u(j\omega)|\sim\mathcal{N}(0,\,2\sigma_0^2(\omega))$. The variance $\sigma_0^2(\omega)=\mathrm{var}[|\widehat{H}_0(j\omega)|]$ is generally unknown, but may be estimated in the baseline phase (Table 4).

Equality of the two FRF magnitudes may be then examined at the selected α (type I) risk level through the statistical test:

$$\begin{aligned} &Z=|\delta|\widehat{H}(j\omega)||/\sqrt{2\widehat{\sigma}_o^2(\omega)}\leq Z_{1-\alpha/2} \quad (\forall\,\omega)\Longrightarrow H_0 \text{ is accepted} \quad \text{(healthy structure)}\\ &\text{Else} \Longrightarrow H_1 \text{ is accepted} \quad \text{(damaged structure),}\end{aligned} \tag{5}$$

with $Z_{1-\alpha/2}$ designating the standard normal distribution's $1-\alpha/2$ critical point.

Damage identification may be similarly achieved by performing hypotheses testing similar to the above for damages from each potential damage type (see Table 3).

Table 4
Estimation of non-parametric statistical time series models.

Quantity	Power spectral density (PSD)	Cross spectral density (CSD)	Frequency response function (FRF)
Estimator	$\widehat{S}_{yy}(\omega)=\frac{1}{K}\sum_{i=1}^{K}\widehat{Y}_L^i(j\omega)\widehat{Y}_L^i(-j\omega)$ $\widehat{Y}_L^i(j\omega)=\frac{1}{\sqrt{L}}\sum_{t=1}^{L}a[t]\widehat{y}^i[t]e^{-j\omega T_s}$ $\widehat{y}^i[t]=y^i[t]-\widehat{\mu}_y$ (i-th segment of length L)	$\widehat{S}_{yx}(\omega)=\frac{1}{K}\sum_{i=1}^{K}\widehat{Y}_L^i(j\omega)\widehat{X}_L^i(-j\omega)$ $\widehat{X}_L^i(j\omega)=\frac{1}{\sqrt{L}}\sum_{t=1}^{L}a[t]\widehat{x}^i[t]e^{-j\omega T_s}$ $\widehat{x}^i[t]=x^i[t]-\widehat{\mu}_x$ (i-th segment of length L)	$\widehat{H}(j\omega)=\widehat{S}_{yx}(j\omega)/\widehat{S}_{xx}(\omega)$
Properties	$2K\widehat{S}_{yy}(\omega)/S_{yy}(\omega)\sim\chi^2(2K)$	$E\{\lvert\widehat{S}_{yx}(j\omega)\rvert\}\approx\lvert S_{yx}(j\omega)\rvert$ $\mathrm{var}[\lvert\widehat{S}_{yx}(j\omega)\rvert]\approx\frac{\lvert S_{yx}(j\omega)\rvert^2}{\gamma^2(\omega)K}$	$E\{\lvert\widehat{H}(j\omega)\rvert\}\approx\lvert H(j\omega)\rvert$ $\mathrm{var}[\lvert\widehat{H}(j\omega)\rvert]\approx\frac{1-\gamma^2(\omega)}{\gamma^2(\omega)2K}$
Comments	 K: number of data segments $a[t]$: time window	Welch method (no overlap) For $N\to\infty$, $a[t]=1$ $\gamma^2(\omega)\to 1$ or $K\to\infty$	

Remarks: $\omega\in[0,2\pi/T_s]$ stands for frequency in radian per second; j stands for the imaginary unit; K stands for the number of segments used in Welch spectral estimation; $\gamma^2(\omega)$ stands for the coherence function [31, p. 196]. The frequency-domain estimator distributions may be approximated as Gaussian for small relative errors (that is $\gamma^2(\omega)\to 1$ or $K\to\infty$) [31, pp. 274–275].
MATLAB functions: *pwelch.m* for $\widehat{S}_{yy}$, *csd.m* for $\widehat{S}_{yx}$, *tfestimate.m* for $\widehat{H}$, *mscohere.m* for $\widehat{\gamma}^2$.

4.2. Parametric methods

4.2.1. A model parameter based method

This method bases damage detection and identification on a characteristic quantity $Q=f(\boldsymbol{\theta})$ which is function of the parameter vector $\boldsymbol{\theta}$ of a parametric time series model ($Q=\boldsymbol{\theta}$ in the typical case).

Let $\widehat{\boldsymbol{\theta}}$ designate a proper estimator of the parameter vector $\boldsymbol{\theta}$ [29,16, pp. 212–213]. For sufficiently long signals the estimator is (under mild assumptions) Gaussian distributed with mean equal to its true value $\boldsymbol{\theta}$ and a certain covariance $\boldsymbol{P}_{\boldsymbol{\theta}}$ [16, p. 303], hence $\widehat{\boldsymbol{\theta}}\sim\mathcal{N}(\boldsymbol{\theta},\boldsymbol{P}_{\boldsymbol{\theta}})$.

Damage detection is based on testing for statistically significant changes in the parameter vector $\boldsymbol{\theta}$ between the nominal and current state of the structure through the hypothesis testing problem [5,6]:

$$\begin{aligned} &H_0: \delta\boldsymbol{\theta}=\boldsymbol{\theta}_o-\boldsymbol{\theta}_u=\mathbf{0} \quad \text{(null hypothesis — healthy structure)},\\ &H_1: \delta\boldsymbol{\theta}=\boldsymbol{\theta}_o-\boldsymbol{\theta}_u\neq\mathbf{0} \quad \text{(alternative hypothesis — damaged structure)}. \end{aligned} \tag{6}$$

The difference between the two parameter vector estimators also follows Gaussian distribution [5], that is $\delta\widehat{\boldsymbol{\theta}}=\widehat{\boldsymbol{\theta}}_o-\widehat{\boldsymbol{\theta}}_u\sim\mathcal{N}(\delta\boldsymbol{\theta},\delta\boldsymbol{P})$, with $\delta\boldsymbol{\theta}=\boldsymbol{\theta}_o-\boldsymbol{\theta}_u$ and $\delta P=\boldsymbol{P}_o+\boldsymbol{P}_u$, where $\boldsymbol{P}_o$, $\boldsymbol{P}_u$ designate the corresponding covariance matrices. Under the null (H_0) hypothesis $\delta\widehat{\boldsymbol{\theta}}=\widehat{\boldsymbol{\theta}}_o-\widehat{\boldsymbol{\theta}}_u\sim\mathcal{N}(\mathbf{0},2\boldsymbol{P}_o)$ and the quantity $\chi^2_{\boldsymbol{\theta}}=\delta\widehat{\boldsymbol{\theta}}^T\cdot\delta\boldsymbol{P}^{-1}\cdot\delta\widehat{\boldsymbol{\theta}}$ (with $\delta\boldsymbol{P}=2\boldsymbol{P}_o$) follows χ^2 distribution with d (parameter vector dimensionality) degrees of freedom [5,6,16, p. 558].

As the covariance matrix $\boldsymbol{P}_o$ corresponding to the healthy structure is unavailable, its estimated version $\widehat{\boldsymbol{P}}_o$ is used. Then, the following test is constructed at the α (type I) risk level:

$$\begin{aligned} &\chi^2_{\boldsymbol{\theta}}\leq\chi^2_{1-\alpha}(d)\Longrightarrow H_0 \text{ is accepted} \quad \text{(healthy structure)}\\ &\text{Else}\Longrightarrow H_1 \text{ is accepted} \quad \text{(damaged structure)}, \end{aligned} \tag{7}$$

with $\chi^2_{1-\alpha}(d)$ designating the χ^2 distribution's $1-\alpha$ critical point.

Damage identification may be based on the multiple hypotheses testing problem of Table 3 comparing the parameter vector $\widehat{\boldsymbol{\theta}}_u$ belonging to the current state of the structure to those corresponding to different damage types $\widehat{\boldsymbol{\theta}}_A$, $\widehat{\boldsymbol{\theta}}_B$, ...

4.2.2. Residual based methods

These methods [5,6] attempt damage detection and identification using characteristic quantities that are functions of residual sequences obtained by driving the current signal(s) Z_u through suitable predetermined—in the baseline phase—models $M_o, M_A, M_B,\ldots$, each one corresponding to a particular state of the structure (healthy and damaged structure under specific damage types). The general idea is that the residual sequence obtained by a model that truly reflects the actual (current) state of the structure will possess certain distinct properties, and will be thus possible to distinguish. An advantage of the methods is that model identification is not repeated in the inspection phase.

Let M_V designate the model representing the structure in its V state ($V=o$ or $V=A, B,\ldots$). The residual series obtained by driving the current signals Z_u through each one of the aforementioned models are designated as $e_{ou}[t]$, $e_{Au}[t]$, $e_{Bu}[t],\ldots$ and

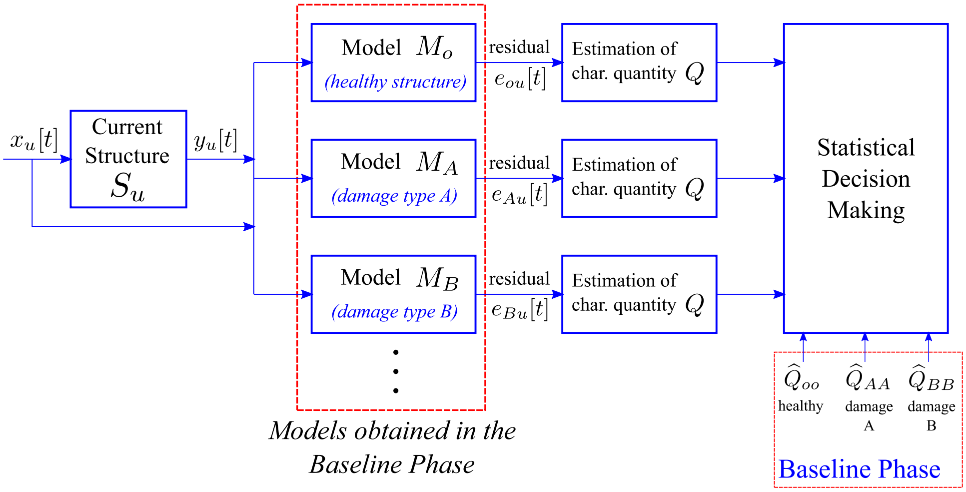

Fig. 3. Schematic for residual based statistical time series methods for SHM (the inspection phase is depicted outside the dashed boxes).

are characterized by respective variances σ^2_{ou}, σ^2_{Au}, σ^2_{Bu}, ... — notice that the first subscript designates the model employed and the second the structural state corresponding to the current excitation and/or response signal(s) used. The characteristic quantities obtained from the corresponding residual series are designated as Q_{ou}, Q_{Au}, Q_{Bu},... . The characteristic quantities obtained using the baseline data records are designated as Q_{VV} ($V{=}o$ or $V{=}A, B, \ldots$).

A schematic for the residual based statistical time series methods for SHM is illustrated in Fig. 3.

4.2.2.1. Residual variance based method. In this method the characteristic quantity is the residual variance. Damage detection is based on the fact that the residual series $e_{ou}[t]$, obtained by driving the current signal(s) Z_u through the model M_o corresponding to the nominal (healthy) structure should be characterized by variance σ^2_{ou}, which becomes minimal (specifically equal to σ^2_{oo}) if and only if the current structure is healthy. The following hypothesis testing problem is then set up:

$$\begin{aligned} &H_0 : \sigma^2_{oo} = \sigma^2_{ou} \quad \text{(null hypothesis — healthy structure)} \\ &H_1 : \sigma^2_{oo} < \sigma^2_{ou} \quad \text{(alternative hypothesis — damaged structure).} \end{aligned} \tag{8}$$

Under the null (H_0) hypothesis the residuals $e_{ou}[t]$ are (just like the residuals $e_{oo}[t]$) iid zero mean Gaussian with variance σ^2_{oo} [5]. Hence, the quantities $N_u\widehat{\sigma}^2_{ou}/\sigma^2_{oo}$ and $(N_o-d)\widehat{\sigma}^2_{oo}/\sigma^2_{oo}$ follow central χ^2 distributions with N_u and N_o-d degrees of freedom, respectively [5]. Note that N_o and N_u designate the number of samples used in estimating the residual variance in the healthy and current cases, respectively (typically $N_o{=}N_u{=}N$), and d designates the dimensionality of the model parameter vector. Consequently, the statistic $\widehat{\sigma}^2_{ou}/\widehat{\sigma}^2_{oo}$ follows F distribution with (N_u, N_o-d) degrees of freedom [5]. The following test is then constructed at the α (type I) risk level:

$$\begin{aligned} &F = \frac{\widehat{\sigma}^2_{ou}}{\widehat{\sigma}^2_{oo}} \le f_{1-\alpha}(N_u, N_o-d) \Longrightarrow H_0 \text{ is accepted} \quad \text{(healthy structure)} \\ &\text{Else} \Longrightarrow H_1 \text{ is accepted} \quad \text{(damaged structure).} \end{aligned} \tag{9}$$

Damage identification may be achieved based on the multiple hypotheses testing problem of Table 3.

4.2.2.2. Likelihood function based method. In this method damage detection is based on the likelihood function under the null (H_0) hypothesis of a healthy structure [5,6,32, pp. 119–120]. The hypothesis testing problem considered is:

$$\begin{aligned} &H_0 : \boldsymbol{\theta}_o = \boldsymbol{\theta}_u \quad \text{(null hypothesis — healthy structure),} \\ &H_1 : \boldsymbol{\theta}_o \neq \boldsymbol{\theta}_u \quad \text{(alternative hypothesis — damaged structure),} \end{aligned} \tag{10}$$

with $\boldsymbol{\theta}_o$, $\boldsymbol{\theta}_u$ designating the parameter vectors corresponding to the healthy and current structure, respectively. Assuming serial independence of the residual sequence, the Gaussian likelihood function $L_y(Y, \boldsymbol{\theta}/X)$ for the data Y given X is obtained [5,6,33, p. 226].

Under the null (H_0) hypothesis, the residual series $e_{ou}[t]$ generated by driving the current signal(s) through the nominal model is (just like $e_{oo}[t]$) iid Gaussian with zero mean and variance σ^2_{oo}. Decision making may be then based on the likelihood function under H_0 evaluated for the current data, by requiring it to be larger or equal to a threshold l (which is to be selected) in order for the null (H_0) hypothesis to be accepted:

$$\begin{array}{l} L_y(Y,\boldsymbol{\theta}_o/X) \geq l \Longrightarrow H_0 \text{ is accepted} \quad \text{(healthy structure)} \\ \text{Else} \Longrightarrow H_1 \text{ is accepted} \quad \text{(damaged structure)}. \end{array} \tag{11}$$

Under the null (H_0) hypothesis, the statistic $N\widehat{\sigma}^2_{ou}/\widehat{\sigma}^2_{oo}$ follows χ^2 distribution with N degrees of freedom [5,6]. This leads to the re-expression of the above decision making rule as follows:

$$\begin{array}{l} \chi^2_N = \dfrac{N\widehat{\sigma}^2_{ou}}{\widehat{\sigma}^2_{oo}} \leq \chi^2_{1-\alpha}(N) \Longrightarrow H_0 \text{ is accepted} \quad \text{(healthy structure)} \\ \text{Else} \Longrightarrow H_1 \text{ is accepted} \quad \text{(damaged structure)}, \end{array} \tag{12}$$

with $\chi^2_{1-\alpha}(N)$ designating the χ^2 distribution's $1-\alpha$ critical point. Note that the above decision making is similar to that of the previous (residual variance based) method.

Damage identification may be achieved by computing the likelihood function for the current signal(s) for the various values of $\boldsymbol{\theta}$ ($\boldsymbol{\theta}_A$, $\boldsymbol{\theta}_B$, ...) and accepting the hypothesis that corresponds to the maximum value of the likelihood.

4.2.2.3. Residual uncorrelatedness based method. This method is based on the fact that the residual sequence $e_{ou}[t]$ obtained by driving the current signal(s) Z_u through the nominal model will be *uncorrelated* (white) if and only if the current structure is in its nominal (healthy) state [5,6]. Damage detection may be then based on the hypothesis testing problem:

$$\begin{array}{l} H_0 : \rho[\tau] = 0, \quad \tau = 1, 2, \ldots, r \quad \text{(null hypothesis — healthy structure)} \\ H_1 : \rho[\tau] \neq 0, \quad \text{for some } \tau \quad \text{(alternative hypothesis — damaged structure)}, \end{array} \tag{13}$$

with $\rho[\tau]$ designating the normalized autocovariance function (see Table 4) of the $e_{ou}[t]$ residual sequence.

Under the null (H_0) hypothesis, $e_{ou}[t]$ is iid Gaussian with zero mean and the statistic $\chi^2_\rho = N(N+2)\sum_{\tau=1}^{r}(N-\tau)^{-1}\widehat{\rho}^2[\tau]$ follows χ^2 distribution with r degrees of freedom and $\widehat{\rho}[\tau]$ designating the estimator of $\rho[\tau]$ [33, p. 314]. Decision making is then based on the following test at the α (type I) risk level:

$$\begin{array}{l} \chi^2_\rho = N(N+2)\displaystyle\sum_{\tau=1}^{r}(N-\tau)^{-1}\widehat{\rho}^2[\tau] \leq \chi^2_{1-\alpha}(r) \Longrightarrow H_0 \text{ is accepted} \quad \text{(healthy structure)} \\ \text{Else} \Longrightarrow H_1 \text{ is accepted} \quad \text{(damaged structure)}. \end{array} \tag{14}$$

Damage identification may be achieved by similarly examining which one of the $e_{Vu}[t]$ (V=A, B,...) residual series is uncorrelated.

5. Experimental assessment of statistical time series methods for SHM

The experimental assessment of the univariate statistical time series methods is based on a number of test cases, each corresponding to a single (out of several possible) structural states (damage scenarios—see Table 1), a single experiment (Table 1), and a single vibration response measurement position (out of Points Y1, Y2, Y3—Fig. 1). Note that 40 experiments are run for the healthy structure and 32 for each considered damage state (damage types A, B,..., E).

In Sections 5.1 and 5.2 representative results for the first vibration measurement position (Point Y1, Fig. 1) are presented, while in Section 5.3 summary results for all three vibration measurement positions are presented.

5.1. Baseline phase: Structural identification under various structural states (measurement position Y1)

5.1.1. Non-parametric methods

Non-parametric identification of the structure is based on N=30 720 ($\approx$120 s) sample-long excitation–response signals. An L=2048 sample-long Hamming data window with zero overlap is used (number of segments K=15) for PSD (MATLAB function *pwelch.m*) and FRF (MATLAB function *tfestimate.m*) Welch based estimation (see Tables 4 and 5).

Table 5
Non-parametric estimation details.

Data length	N=30 720 samples ($\approx$120 s)
Method	Welch
Segment length	L=2048 samples
No of non-overlapping segments	K=15 segments
Window type	Hamming
Frequency resolution	$\Delta f = 0.125$ Hz

The obtained response PSD and FRF magnitude estimates for the healthy and damaged states of the structure (Point Y1) are depicted in Fig. 4. As it may be observed, the healthy and damaged curves are rather similar in the 0.5–30 Hz range, where the first 12 modes are included. Significant differences between the healthy and damage types C, D and E curves are seen in the 30–58 Hz range, where the next 3 modes are included. Finally, discrepancies are more evident for damage types C and E in the 58–100 Hz range, where the next 8 modes are included.

The data sets used for obtaining the above response PSD and FRF estimates for the healthy and damaged structural states are considered as the only baseline (reference) data sets throughout this work and are used for obtaining the nominal characteristic quantities Q_o for each time series method. The healthy baseline data set is used for the damage detection task, while the damaged baseline data sets are used for the damage identification task.

5.1.2. Parametric methods

Parametric identification of the structural dynamics is based on $N = 10\,000$ (≈ 39 s) sample-long excitation and single response signals which are used for estimating AutoRegressive with eXogenous excitation (ARX) models (MATLAB function *arx.m*). The modeling strategy consists of the successive fitting of ARX(na, nb) models (with na, nb designating the AR and X orders, respectively; in this study $na = nb = n$) until a suitable model is selected. Model parameter estimation is achieved by minimizing a quadratic prediction error (PE) criterion leading to a least squares (LS) estimator [29,16, p. 206]. Model order selection, which is crucial for successful identification, may be based on a combination of tools, including the Bayesian information criterion (BIC) (Fig. 5a), which is a statistical criterion that penalizes model complexity (order) as a counteraction to a decreasing quality criterion [29,16, pp. 505–507], monitoring of the RSS/SSS (residual sum of squares/ signal sum of squares) criterion (Fig. 5b), monitoring of the residual autocorrelation function (MATLAB function *autocorr.m*)

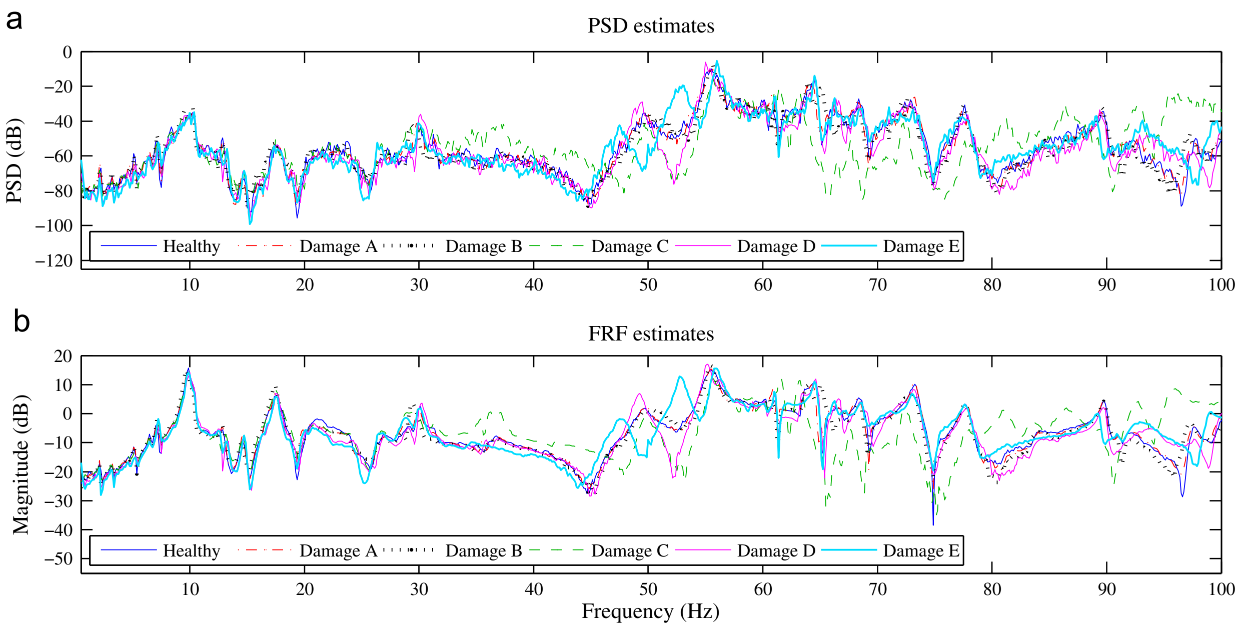

Fig. 4. (a) Power spectral density (PSD) and (b) frequency response function (FRF) magnitude estimates for the healthy and damaged structural states (response Y1).

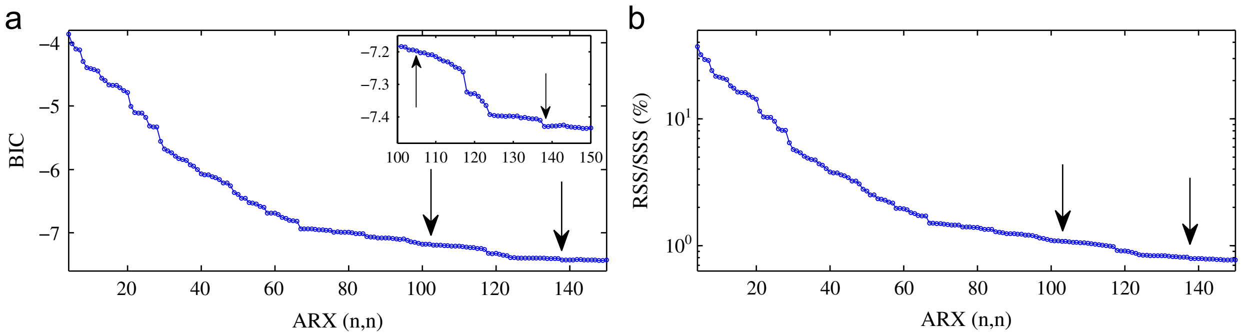

Fig. 5. Order selection criteria for ARX(n, n) type parametric models in the healthy case (response Y1): (a) BIC and (b) RSS/SSS.

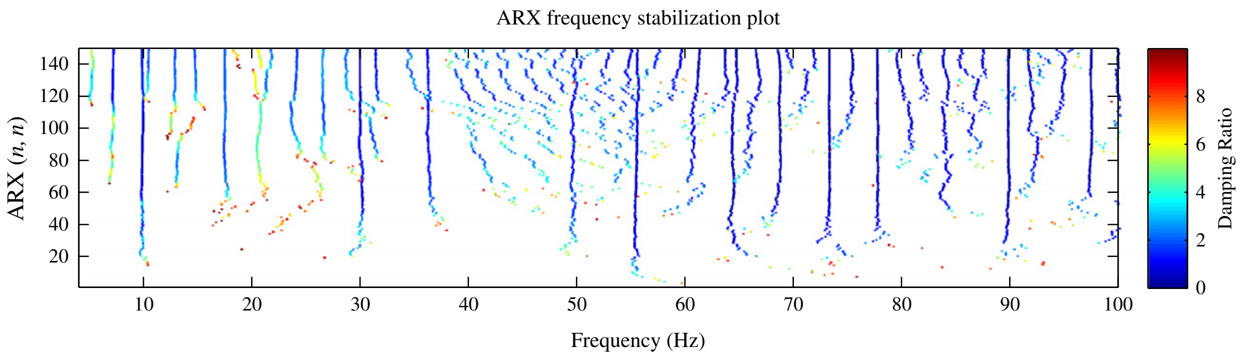

Fig. 6. Frequency stabilization diagram for ARX(n, n) type models in the healthy case (response Y1).

Table 6
Selected models and estimation details (response Y1).

Method	Selected model	Number of estimated parameters	Samples per parameter
Model parameter	ARX(103,103)	207 parameters	48.3
Residual variance	ARX(103,103)	207 parameters	48.3
Residual likelihood	ARX(103,103)	207 parameters	48.3
Residual uncorrelatedness	ARX(138,138)	277 parameters	36.1

Parameter estimation method: weighted least squares (WLS), QR implementation, N=10 000 samples.

[16, p. 512], and use of "stabilization diagrams" (Fig. 6) which depict the estimated modal parameters (usually frequencies) as a function of increasing model order [16,29].

An approximate plateau in the BIC and RSS/SSS sequences is achieved for model order $n>70$ (Fig. 5). Furthermore, as indicated in the frequency stabilization diagram of Fig. 6, model orders of $n>90$ are adequate for most natural frequencies to get stabilized. Notice the color bar in Fig. 6, which demonstrates the damping ratios for each frequency for increasing model order. In the 0.5–50 Hz range, higher damping ratios for model order $n<100$ are observed for certain structural modes.

The above identification procedure leads to an ARX(103,103) model (vibration measurement position Y1), which is selected as adequate for the model parameter, residual variance, and likelihood function based methods. The identified ARX(103,103) representation has 207 parameters with the sample per parameter (SPP) number being equal to 48.3. For the residual uncorrelatedness based method an ARX(138,138) model is selected, as the corresponding model residuals need to be as white as possible in order for the method to work effectively. The identified ARX(138,138) representation has 277 parameters (SPP=36.1). The selected models and estimation details are summarized in Table 6. Note that the identification procedure generally leads to different ARX models (including somewhat different model orders) for each vibration measurement position.

5.2. *Inspection phase (measurement position Y1)*

5.2.1. *PSD based method*

Typical PSD based damage detection results are presented in Fig. 7. Evidently, correct detection at the $\alpha = 10^{-4}$ risk level is obtained in each case, as the test statistic is shown not to exceed the critical points (dashed horizontal lines) in the healthy case, while it exceeds them in the damaged cases. Observe that damage types C (two bolts loosened) and D (one bolt loosened) are easiest to detect (note the logarithmic scale on the vertical axis of Fig. 7), while damage type A (one bolt loosened) is hardest (the test statistic is within the critical points for most frequencies).

Representative damage identification results at the $\alpha = 10^{-4}$ risk level are presented in Fig. 8, with the actual damage being of type A. When testing the hypothesis of damage type A, the test statistic does not exceed the critical points, while it clearly does so when testing the hypothesis of any other damage type.

5.2.2. *FRF based method*

Fig. 9 presents typical FRF based damage detection results. Evidently, correct detection at the $\alpha = 10^{-5}$ risk level is achieved in each case, as the test statistic is shown not to exceed the critical points (dashed horizontal lines) in the healthy case, while it exceeds them in the damaged cases. Again, damage types C and D appear as easiest to detect, while damage types A and B are hardest.

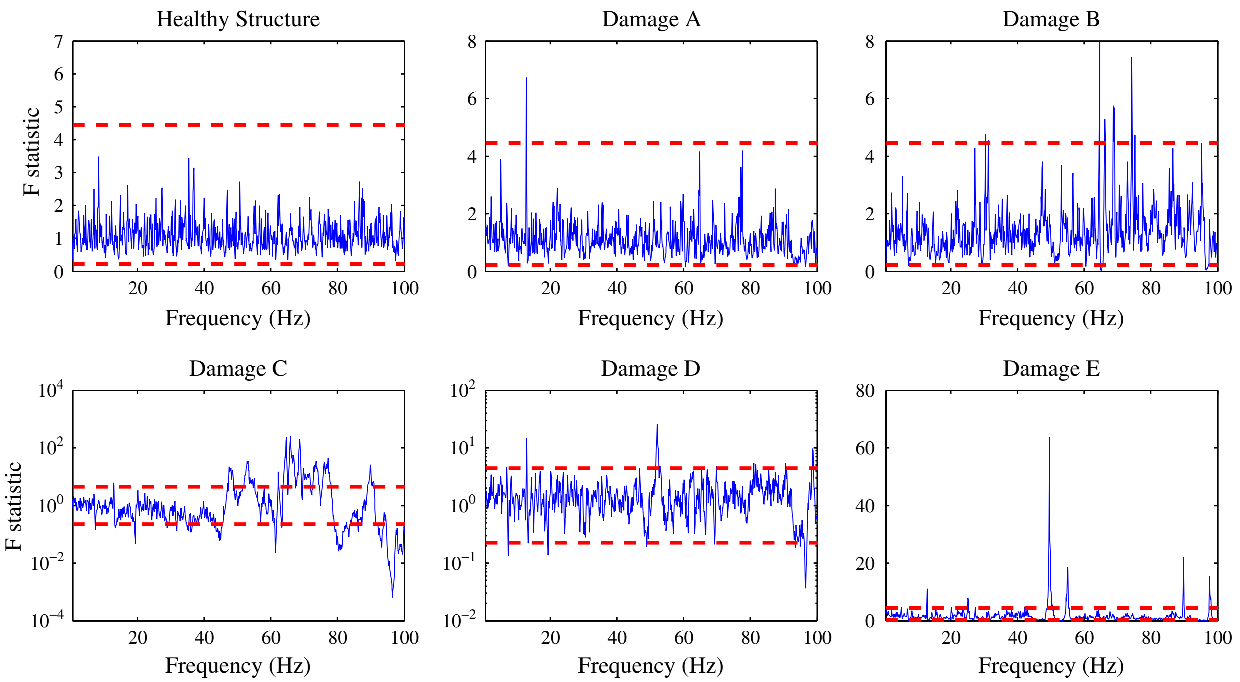

Fig. 7. PSD based method (response Y1): indicative damage detection results for six representative test cases (one healthy and five damaged) at the $\alpha=10^{-4}$ risk level. The actual structural state is shown above each plot box. A damage is detected if the test statistic exceeds the critical points (dashed horizontal lines).

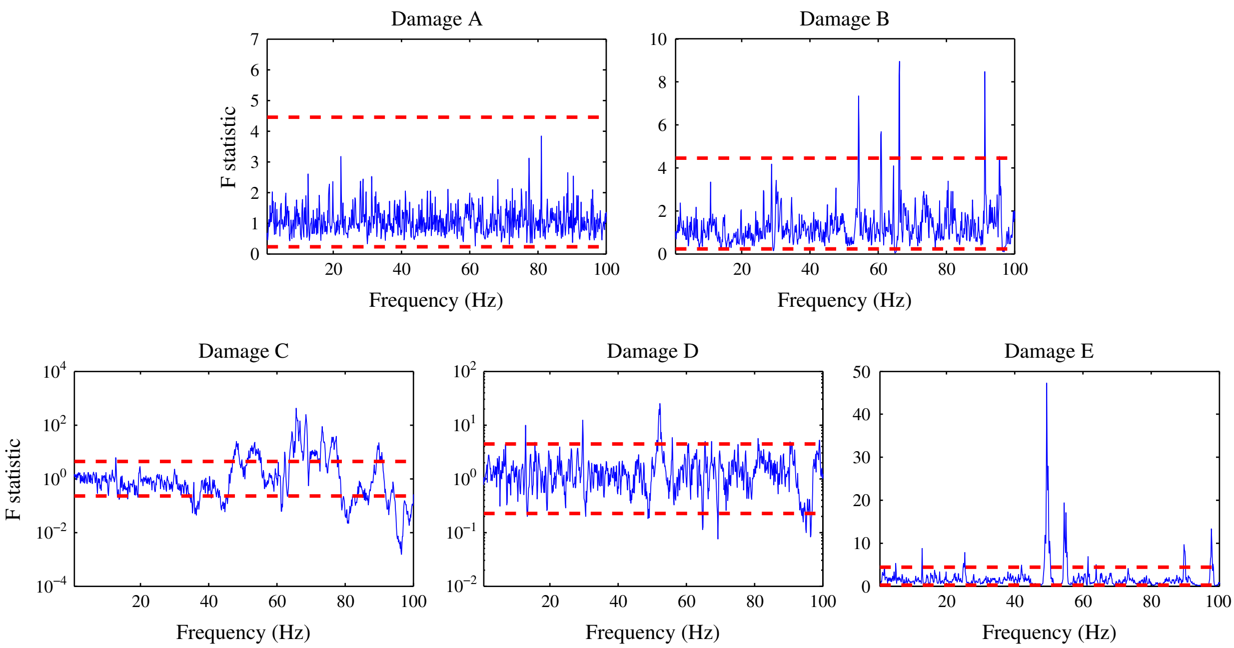

Fig. 8. PSD based method (response Y1): indicative damage identification results for five damage test cases at the $\alpha=10^{-4}$ risk level, with the actual damage being of type A. Each considered test case is shown above each plot box. A damage type is identified as current when the test statistic does not exceed the critical points (dashed horizontal lines).

Indicative damage identification results at the $\alpha=10^{-5}$ risk level are presented in Fig. 10, with the actual damage being of type C. When testing the hypothesis of damage type C, the test statistic does not exceed the critical points, while it clearly does so when testing the hypothesis of any other damage type.

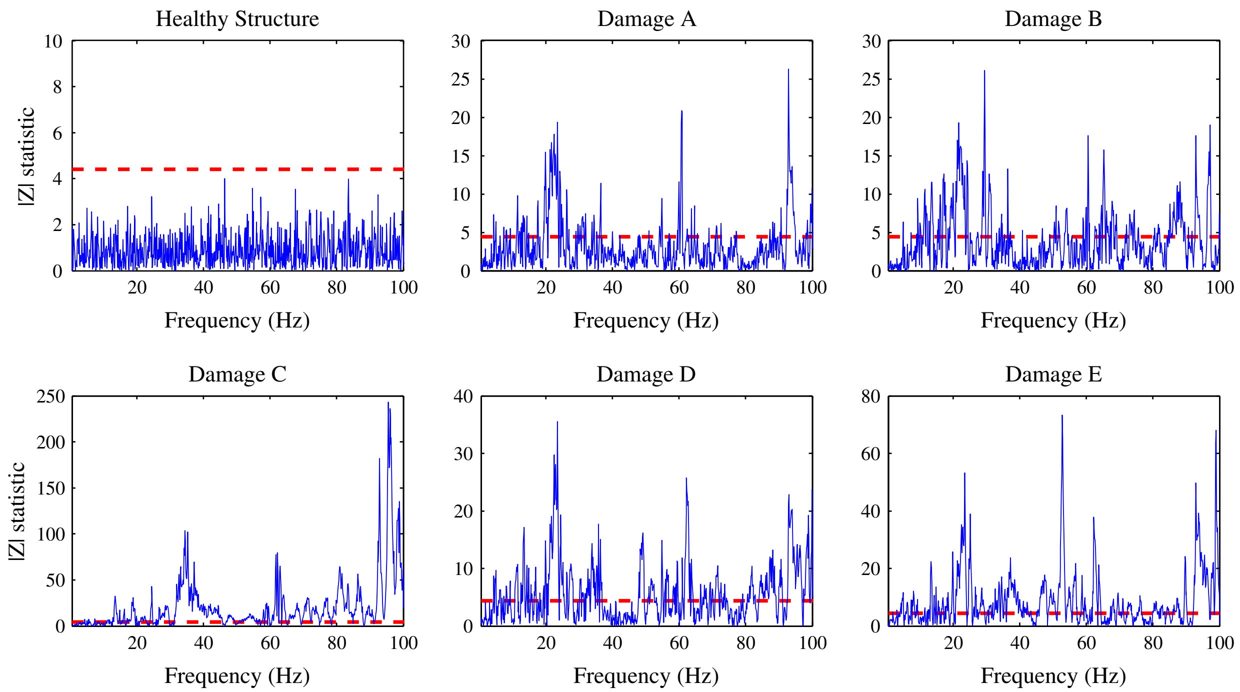

Fig. 9. FRF magnitude based method (response Y1): indicative damage detection results for six representative test cases (one healthy and five damaged) at the $\alpha = 10^{-5}$ risk level. The actual structural state is shown above each plot box. A damage is detected if the test statistic exceeds the critical points (dashed horizontal lines).

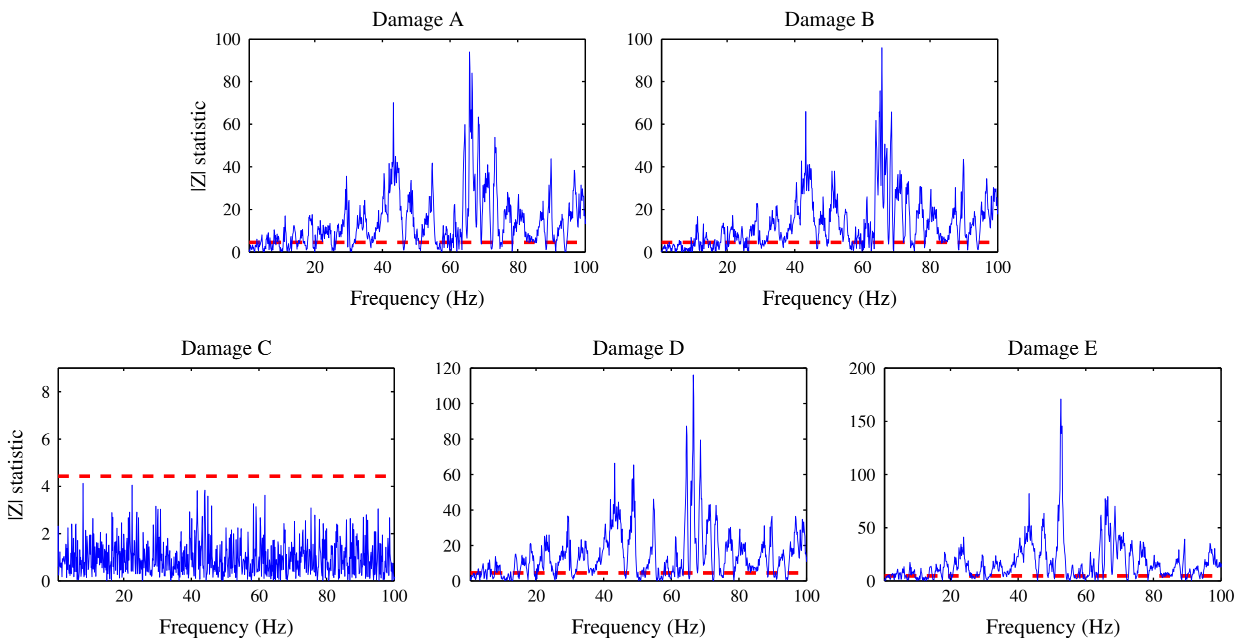

Fig. 10. FRF magnitude based method (response Y1): indicative damage identification results for five damage test cases at the $\alpha = 10^{-5}$ risk level, with the actual damage being of type C. Each considered test case is shown above each plot box. A damage type is identified as current when its test statistic does not exceed the critical points (dashed horizontal lines).

5.2.3. Model parameter based method

The model parameter based method (excitation–response case) is based on the identified ARX(103,103) models from the baseline phase, as well as on identified ARX(103,103) models from the current (unknown) data records Z_u (inspection phase).

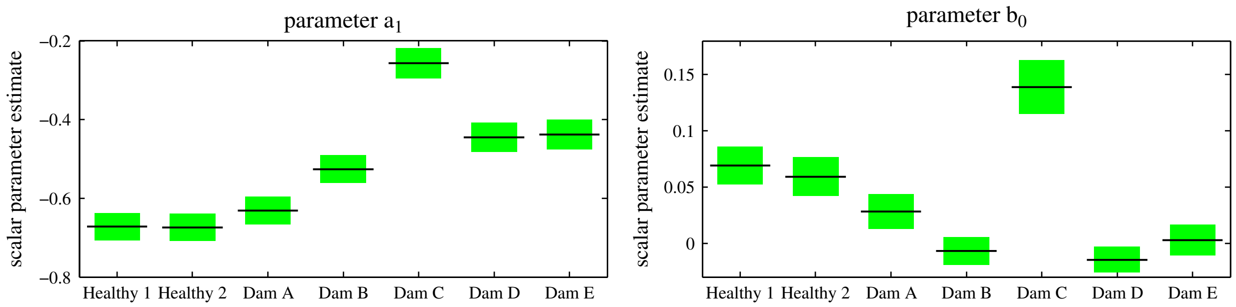

Fig. 11. Model parameter based method (response Y1): model parameter estimates for two healthy and five damage states (the dark lines represent point estimates and the shaded boxes ± 3 sample standard deviation confidence intervals).

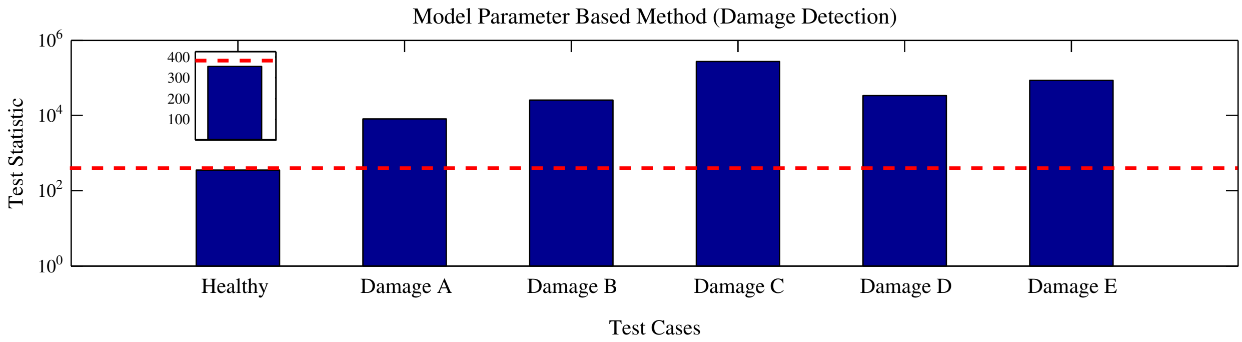

Fig. 12. Model parameter based method (response Y1): indicative damage detection results for six representative test cases (one healthy and five damaged) at the $\alpha = 10^{-12}$ risk level. A damage is detected if the test statistic (bar) exceeds the critical point (dashed horizontal line).

Fig. 11 depicts typical scalar model parameter estimates (a_1 and b_o) based on ARX(103,103) models for two healthy and five damaged states of the structure. The dark lines represent the scalar parameter estimates for each test case, while the shaded boxes designate their corresponding ± 3 sample standard deviation confidence intervals. It may be observed that the parameter estimates obtained from models representing damaged structural states significantly differ from the parameter estimates obtained from healthy models. Moreover, the interval estimates obtained from the healthy models overlap, implying rather small changes.

Figs. 12 and 13 present typical parametric damage detection and identification results, respectively, obtained by the model parameter based method at the $\alpha = 10^{-12}$ risk level. Evidently, correct detection (Fig. 12) is obtained in each case, as the test statistic is shown not to exceed the critical point in the healthy case, while it exceeds it in the damaged cases; note the logarithmic scale on the vertical axis which indicates significant difference between the healthy and damaged test statistics. Moreover, Fig. 13 demonstrates the ability of the method to accurately identify the actual damage type.

5.2.4. Residual based methods

5.2.4.1. Residual variance based method. This method tackles damage detection and identification based on the identified (in the baseline phase) ARX(103,103) models–no model identification is involved in the inspection phase. Fig. 14 depicts typical residual variance estimates based on ARX(103,103) models for two healthy and five damaged states of the structure. The dark lines represent the scalar residual variance estimates for each test case, while the shaded boxes designate their corresponding ± 3 standard deviation confidence intervals. The residual variances $\widehat{\sigma}^2_{ou}, \widehat{\sigma}^2_{Au}, \ldots, \widehat{\sigma}^2_{Eu}$, corresponding to each test case, are estimated from the respective residual sequences $e_{ou}[t], e_{Au}[t], \ldots, e_{Eu}[t]$ obtained by driving the current (unknown) signals Z_u through the models $M_o, M_A, \ldots, M_E$, respectively.

As it may be observed, the residual variance interval estimates $\widehat{\sigma}^2_{ou}$ obtained from the two healthy data sets are quite close and overlap. On the other hand, the variance estimates $\widehat{\sigma}^2_{Au}, \ldots, \widehat{\sigma}^2_{Eu}$ obtained from representative damaged data sets are significantly greater than the healthy estimates (interval estimates are clearly separated). Notice that the more severe damage types (such as types C and E) yield greater residual variance estimates than the less severe ones (damage types A and B).

Typical damage detection and identification results are presented in Figs. 15 and 16, respectively, at the $\alpha = 10^{-12}$ risk level. Evidently, correct detection (Fig. 15) is obtained in each considered case, as the test statistic is shown not to exceed the critical point in the healthy case, while it exceeds it in the damaged test cases. Moreover, Fig. 16 demonstrates the ability of the method to correctly identify the actual damage type (note the logarithmic scale on the vertical axes).

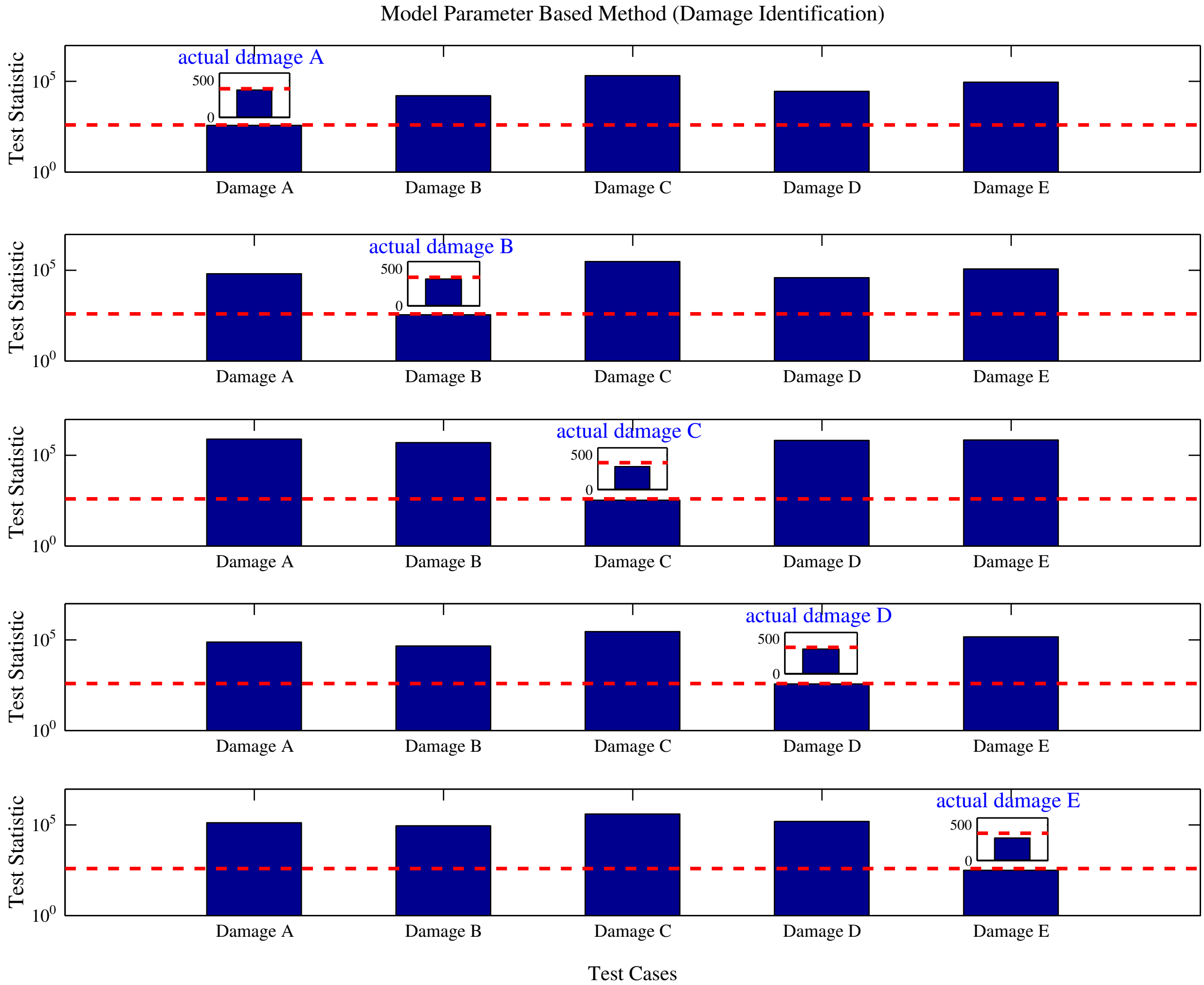

Fig. 13. Model parameter based method (response Y1): indicative damage identification results for five damage test cases at the $\alpha = 10^{-12}$ risk level. Each bar corresponds to each considered hypothesis test, with the actual damage indicated within each subplot. A damage type is identified as current if the test statistic (bar) does not exceed the critical point (dashed horizontal line).

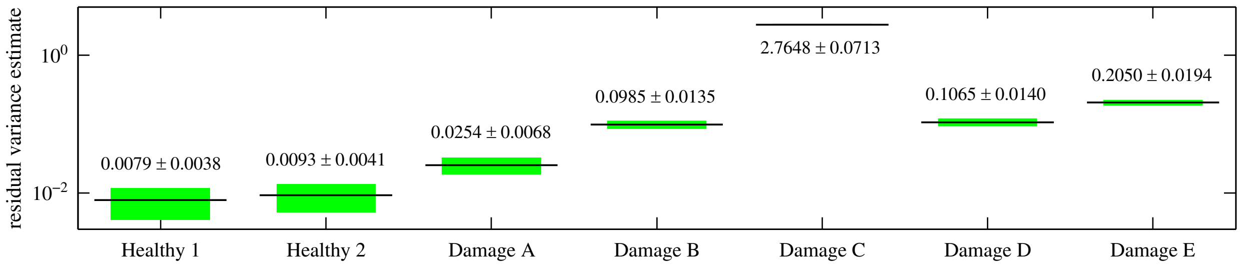

Fig. 14. Residual variance based method (response Y1): residual variance estimates based on ARX(103,103) models for two healthy and five damaged states (the dark lines represent point variance estimates and the shaded boxes ± 3 sample standard deviation confidence intervals).

The residual variance and likelihood function based methods exhibit quite identical performance, as the data record length N is large. This is expected and rather obvious from the comparison of Eqs. (9) and (12). Hence, for the sake of brevity, the results for the likelihood function based method are omitted.

5.2.4.2. Residual uncorrelatedness based method. This method tackles damage detection and identification based on the identified (in the baseline phase) ARX(138,138) models. Fig. 17 depicts typical residual normalized ACF estimates $\widehat{\rho}[\tau]$ for the first four lags ($\tau = 1, \ldots, 4$), based on ARX(138,138) models for the healthy and five damaged structural states.

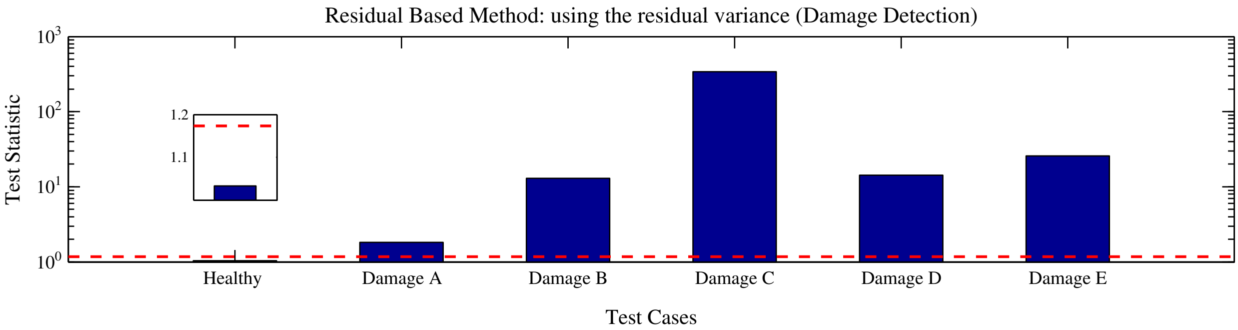

Fig. 15. Residual variance based method (response Y1): indicative damage detection results for six representative test cases (one healthy and five damaged) at the $\alpha = 10^{-12}$ risk level. A damage is detected if the test statistic (bar) exceeds the critical point (dashed horizontal line).

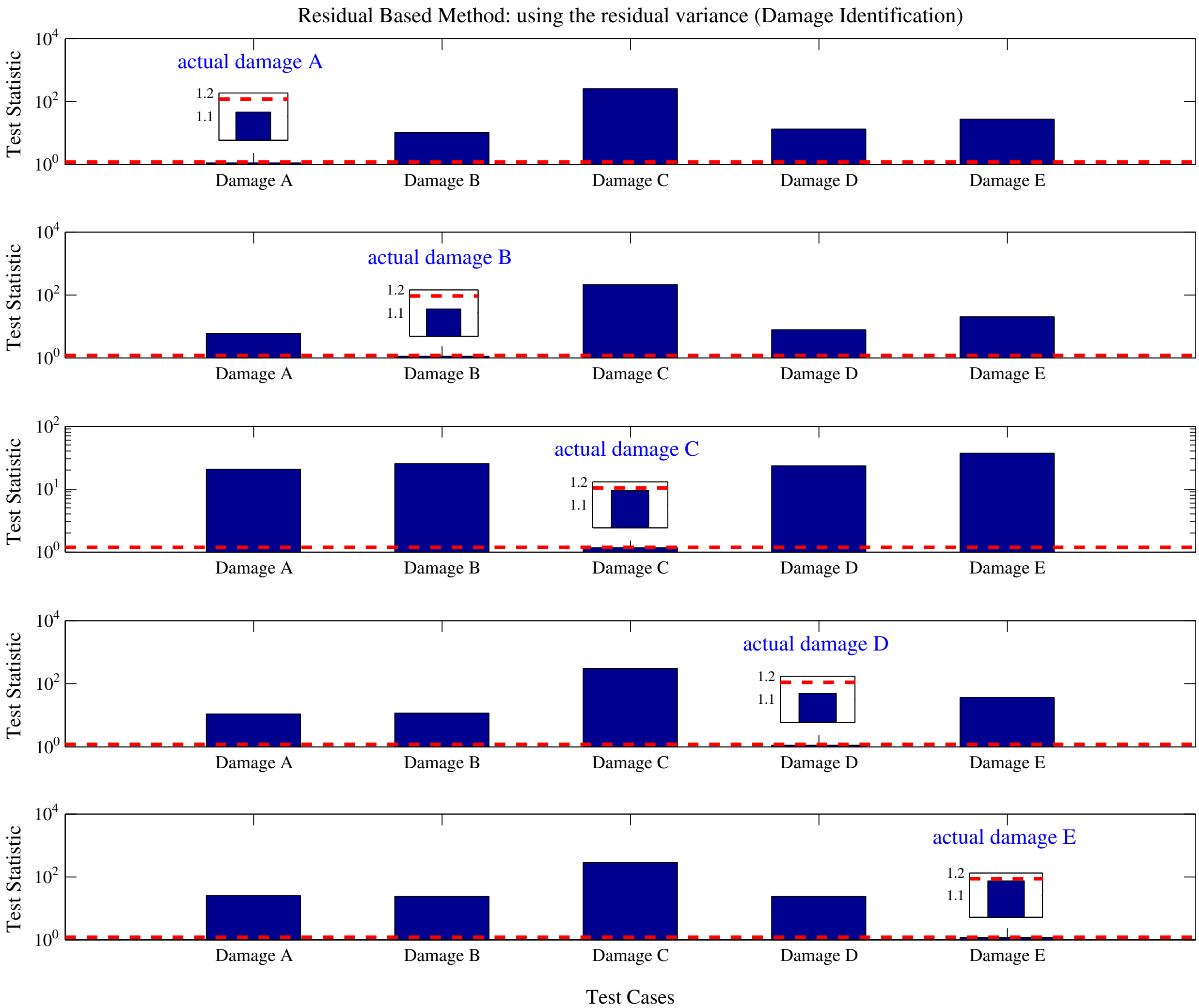

Fig. 16. Residual variance based method (response Y1): indicative damage identification results for five damage test cases at the $\alpha = 10^{-12}$ risk level. Each bar corresponds to each considered hypothesis test, with the actual damage indicated within each subplot. A damage type is identified as current if the test statistic (bar) does not exceed the critical point (dashed horizontal line).

The residuals for each considered state of the structure are obtained by driving the current data records Z_u through the models $M_o, M_A, \ldots, M_E$. Under the null hypothesis of a healthy current structure, the first residual series (obtained by driving the signals through the model M_o) normalized ACF estimates should lie within the statistical insignificance zone of $\pm 1.96/\sqrt{N}$

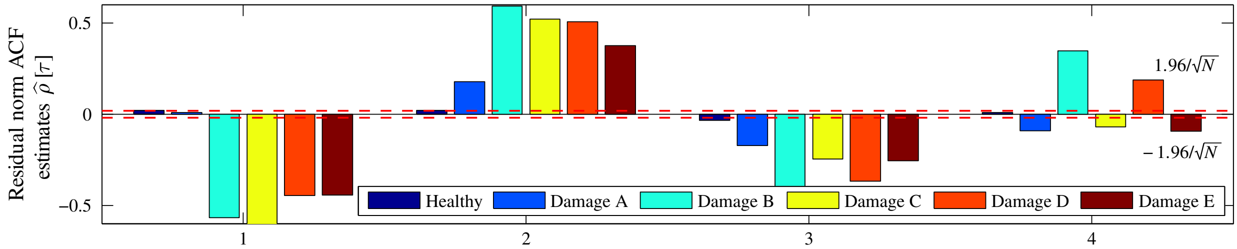

Fig. 17. Residual uncorrelatedness based method (response Y1): normalized residual ACF estimates $\hat{\rho}[\tau]$ based on ARX(138,138) models for one healthy and five damaged states. The dashed horizontal lines designate the limits within which the ACF can be accepted as being zero at the $\alpha = 0.05$ risk level.

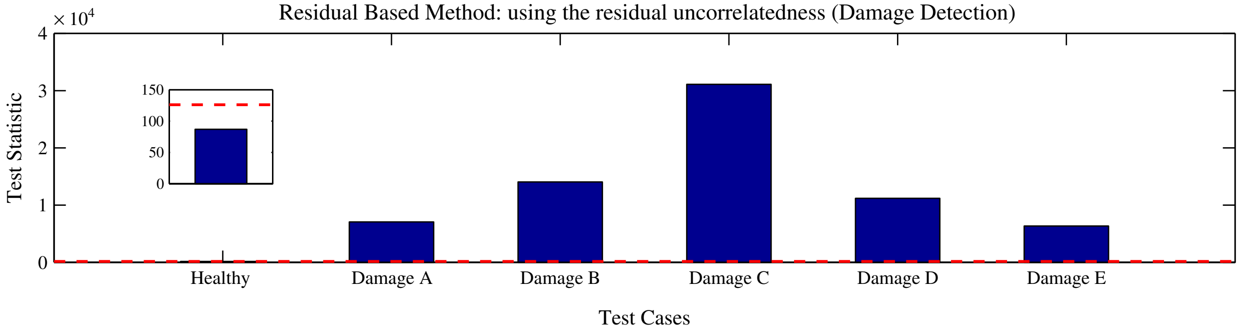

Fig. 18. Residual uncorrelatedness based method (response Y1): indicative damage detection results for six representative test cases (one healthy and five damaged) at the $\alpha = 10^{-12}$ risk level (max lag r=25). A damage is detected if the test statistic (bar) exceeds the critical point (dashed horizontal line).

with probability p=0.95. This should not be the case for the other residual series (obtained by driving the signals through the each one of the $M_A, \ldots, M_E$ models).

Representative damage detection and identification results via the residual uncorrelatedness based method are, at the $\alpha = 10^{-12}$ risk level with r=25 (see Eq. (14)), presented in Figs. 18 and 19, respectively. Evidently, correct detection (Fig. 18) is obtained in each case, as the test statistic is shown not to exceed the critical point in the healthy case, while it exceeds it in the damaged test cases. Moreover, Fig. 19 demonstrates the ability of the method to accurately identify the actual damage type as the current one.

5.3. Summary results and discussion (all measurement positions)

Summary results for all test cases—which also include all three measurement positions (Y1, Y2 and Y3)—are presented in Table 7. Both non-parametric and parametric methods achieve accurate damage detection with almost always zero false alarms for the selected risk levels. In fact only the FRF based method exhibits one and two false alarms for vibration measurement positions Y1 and Y3, respectively. Moreover, the ability of the methods to effectively detect damage is demonstrated by the fact that no missed damage cases are observed. The damage identification results demonstrate the ability of the methods to accurately identify the actual damage type. No damage misclassification cases are observed, except for the FRF based method where misclassification errors occur for damage type A (Table 7).

It is also important to note that the methods are capable of detecting and identifying damage using a single response signal. This is true for the cases where the damage location is relatively close to the response sensor, but also to the cases where the damage location is far from that. Performance is of course, and expectedly, affected by this distance, and this is also shown in the damage type A case where the lowest misclassification rate occurs for sensor Y2 (Table 7) which is closest to the damage location.

Overall, both non-parametric and parametric statistical time series methods demonstrate high potential for effective damage detection and identification based even on a single vibration response signal. Between the two non-parametric methods, the FRF based one appears to achieve better damage detection and identification. Among the parametric methods, the residual based methods appear to achieve clearer damage detection and identification than the parameter based method.

Nevertheless, a number of issues require some attention on part of the user. First, careful model identification—especially in the parametric case—is crucial for successful damage diagnosis. Parametric models require accurate parameter estimation and appropriate model structure (order) selection in order to properly represent the structural dynamics and be effectively used for damage detection and identification. Therefore, parametric methods require adequate user expertise and are somewhat more elaborate than their non-parametric counterparts. In particular, extra attention should be paid to

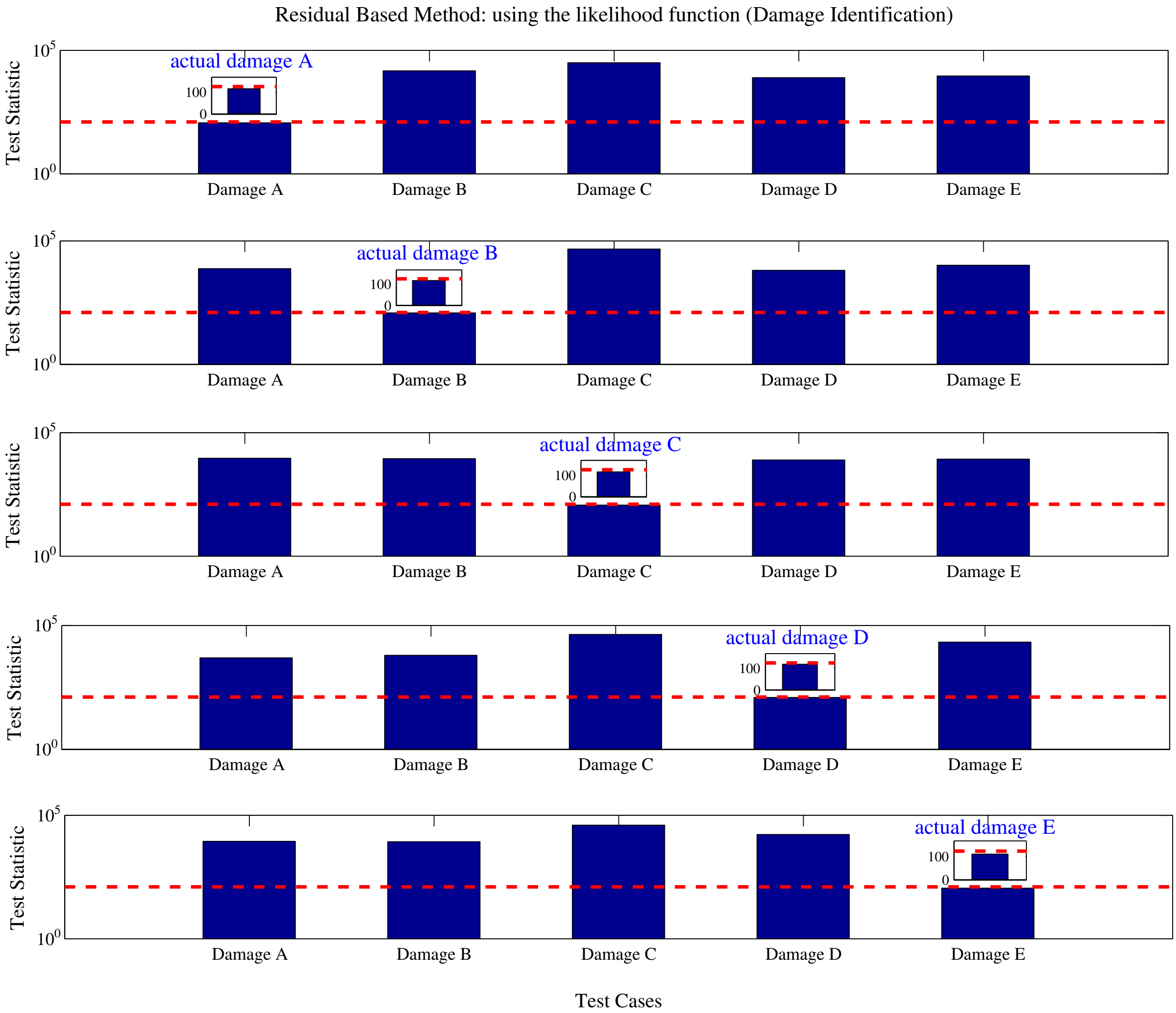

Fig. 19. Residual uncorrelatedness based method (response Y1): indicative damage identification results for five damage test cases at the $\alpha = 10^{-12}$ risk level (max lag r=25). Each bar corresponds to each considered hypothesis test, with the actual damage indicated within each subplot. A damage type is identified as current if the test statistic (bar) does not exceed the critical point (dashed horizontal line).

successful model identification in conjunction with the model residual uncorrelatedness method, as the corresponding model residuals should be as close to whiteness as possible in order for the method to work effectively.

Another issue of primary importance is the proper selection of the risk level α (type I error), for reasons associated with the methods' robustness and effectiveness. If this is not properly adjusted, damage diagnosis will be ineffective, as false alarm, missed damage, and damage misclassification cases may occur. The user is advised to make an initial investigation of the false alarm rates for different α levels using several healthy data sets. Afterwards, potential missed damage cases may be checked with data corresponding to various damaged structural states. When applying the model residual uncorrelatedness based method, the user should be aware of the fact that the max lag r value may also affect performance. Thus, a tentative inquiry on the way max lag r value affects false alarm occurrence should be undertaken. Depending on the exact type and order of the parametric model used, max lag r values may range from a few to $N/4$ (N is the residual signal length in samples).

Moreover, in order for most parametric methods to work effectively, a very small value of type I risk level α is often needed. This is due to the fact that the current parametric time series models (ARMA, ARX, state space and so on) used for modeling the structural dynamics are incapable of fully capturing the experimental, operational and environmental uncertainties that the structure is subjected to—in this context see Refs. [34,35]. For this reason, a very small α is often selected in order to compensate for the lack of effective uncertainty modeling. This subject, along with more accurate modeling of uncertainties, is important for current and future research.

Table 7
Damage detection and identification summary results for three responses (Y1, Y2 and Y3).

Method	Damage detection					
	False alarms	Missed damage				
		Damage A	Damage B	Damage C	Damage D	Damage E
PSD based	0/0/0	0/0/0	0/0/0	0/0/0	0/0/0	0/0/0
FRF based	**1**/0/**2**	0/0/0	0/0/0	0/0/0	0/0/0	0/0/0
Mod. parameter[a]	0/0/0	0/0/0	0/0/0	0/0/0	0/0/0	0/0/0
Res. variance[a]	0/0/0	0/0/0	0/0/0	0/0/0	0/0/0	0/0/0
Res. likelihood[a]	0/0/0	0/0/0	0/0/0	0/0/0	0/0/0	0/0/0
Res. uncorrelatedness[a]	0/0/0	0/0/0	0/0/0	0/0/0	0/0/0	0/0/0

Method	Damage identification				
	Damage misclassification				
	Damage A	Damage B	Damage C	Damage D	Damage E
PSD based	0/0/0	0/0/0	0/0/0	0/0/0	0/0/0
FRF based	**2**/1/**2**	0/0/0	0/0/0	0/0/0	0/0/0
Mod. parameter[a]	0/0/0	0/0/0	0/0/0	0/0/0	0/0/0
Res. variance[a]	0/0/0	0/0/0	0/0/0	0/0/0	0/0/0
Res. likelihood[a]	0/0/0	0/0/0	0/0/0	0/0/0	0/0/0
Res. uncorrelatedness[a]	0/0/0	0/0/0	0/0/0	0/0/0	0/0/0

False alarms for Points Y1/Y2/Y3 out of 39 test cases each.
Missed damages for Points Y1/Y2/Y3 out of 31 test cases each.
Damage misclassification for Points Y1/Y2/Y3 out of 31 test cases each.
[a] Adjusted α.

The selection of the number and position of measurement sensors is another important issue. Several vibration based damage diagnosis techniques that appear to work well in test cases may perform poorly when subjected to the measurement constraints imposed by actual testing [2,3]. Techniques that are to be seriously considered for implementation in the field should demonstrate that they can perform well under limitations of a small number of measurement positions and under the constraint that these positions should be selected a priori, without a priori knowledge of the damage location. As already demonstrated, statistical time series methods are capable of treating damage diagnosis based on limited or even on a single pair of excitation–response measurements and may also achieve a certain level of automation, although their performance on large scale structures needs to be further investigated.

Finally, in the case of multiple damage scenarios, or even single damage cases not considered in the baseline (training) phase, statistical time series methods are capable of effectively treating the damage detection subproblem. The damage identification (classification) subproblem is clearly more difficult, and requires the use of advanced methods, such as those more recently developed by the authors and their co-workers [9,10]. Work on these methods is still on-going, and experimental comparisons along with full assessments are to be made.

6. Concluding remarks

A comparative experimental assessment of vibration based statistical time series methods for SHM was presented via their application to damage diagnosis in a lightweight aluminum truss structure. Some of the important conclusions drawn from this study may be summarized as follows:

- Statistical time series methods for SHM achieve damage detection and identification based on (i) *scalar* or *vector* random excitation and/or vibration response signals, (ii) statistical model building, and (iii) statistical decision making under uncertainty.
- Both non-parametric and parametric methods were shown to effectively tackle damage detection and identification, with parametric methods achieving excellent performance with zero (in the present study) false alarm, missed damage, and damage misclassification rates.
- Both non-parametric and parametric methods were shown to have global damage detection capability, as they are able to detect “local” and “remote” damage with respect to the sensor position used.

- All methods were shown to be capable of correctly identifying the actual damage type, with the exception of the FRF based method which exhibited a small number of damage misclassification errors for damage type A, irrespectively of the vibration measurement position used.
- Parametric time series methods are more elaborate and demand increased user expertise compared to their generally simpler non-parametric counterparts. Yet, they were shown to offer increased sensitivity and accuracy.
- The availability of data records corresponding to various potential damage scenarios is necessary in order to treat damage identification. This may not be possible with the actual structure itself, but laboratory scale models or analytical (finite element) models may be used for this purpose.
- The extension of the methods to the more general *multivariate* case requires the use of corresponding vector models and multivariate statistical decision making procedures and needs to be fully investigated in the future.
- The need for methods capable of working under varying operational and environmental conditions and uncertainties is important and also the subject of current research (for instance [35,36]).

Appendix A. Important conventions and symbols

Bold-face upper/lower case symbols designate matrix/column-vector quantities, respectively. Matrix transposition is indicated by the superscript^T.

A functional argument in parentheses designates function of a real variable; for instance $x(t)$ is a function of analog time $t \in \mathbb{R}$.

A functional argument in brackets designates function of an integer variable; for instance $x[t]$ is a function of normalized discrete time ($t=1, 2, \ldots$). The conversion from discrete normalized time to analog time is based on $(t-1)T_s$, with T_s designating the sampling period.

A functional argument including the imaginary unit designates complex function; for instance $X(j\omega)$ is a complex function of ω.

A hat designates estimator/estimate of the indicated quantity; for instance $\widehat{\boldsymbol{\theta}}$ is an estimator/estimate of $\boldsymbol{\theta}$.

The subscripts "o" and "u" designate quantities associated with the nominal (healthy) and current (unknown) state of the structure, respectively.

Appendix B. Acronyms

ACF	autoCovariance function
ARX	autoRegressive with eXogenous excitation models
BIC	Bayesian information criterion
CSD	cross spectral density
FE	finite element
FRF	frequency response function
iid	identically independently distributed
LS	least squares
PE	prediction error
PSD	power spectral density
RSS	residual sum of squares
SHM	structural health monitoring
SSS	signal sum of squares
WLS	weighted least squares

References

[1] C. Farrar, S. Doebling, D. Nix, Vibration-based structural damage identification, The Royal Society—Philosophical Transactions: Mathematical, Physical and Engineering Sciences 359 (2001) 131–149.
[2] S. Doebling, C. Farrar, M. Prime, D. Shevitz, Damage identification and health monitoring of structural and mechanical systems from changes in their vibration characteristics: a literature review, Technical Report LA-13070-MS, Los Alamos National Laboratory, 1996.
[3] S. Doebling, C. Farrar, M. Prime, A summary review of vibration-based damage identification methods, Shock and Vibration Digest 30 (2) (1998) 91–105.
[4] D. Montalvão, N. Maia, A. Ribeiro, A summary review of vibration-based damage identification methods, Shock and Vibration Digest 38 (4) (2006) 295–324.
[5] S. Fassois, J. Sakellariou, Time series methods for fault detection and identification in vibrating structures, The Royal Society—Philosophical Transactions: Mathematical, Physical and Engineering Sciences 365 (2007) 411–448.
[6] S. Fassois, J. Sakellariou, Statistical time series methods for structural health monitoring, in: C. Boller, F.K. Chang, Y. Fujino (Eds.), Encyclopedia of Structural Health Monitoring, John Wiley & Sons Ltd., Chichester, UK, 2009, pp. 443–472.
[7] M. Basseville, L. Mevel, M. Goursat, Statistical model-based damage detection and localization: subspace-based residuals and damage-to-noise sensitivity ratios, Journal of Sound and Vibration 275 (2004) 769–794.
[8] L. Mevel, M. Goursat, M. Basseville, Stochastic subspace-based structural identification and damage detection and localisation—application to the z24 bridge benchmark, Mechanical Systems and Signal Processing 17 (1) (2003) 143–151.

[9] J. Sakellariou, S. Fassois, Vibration based fault detection and identification in an aircraft skeleton structure via a stochastic functional model based method, Mechanical Systems and Signal Processing 22 (2008) 557–573.
[10] F. Kopsaftopoulos, S. Fassois, Vibration-based structural damage detection and precise assessment via stochastic functionally pooled models, Key Engineering Materials 347 (2007) 127–132.
[11] J. Bodeux, J. Golinval, Application of armav models to the identification and damage detection of mechanical and civil engineering structures, Smart Materials and Structures 10 (2001) 479–489.
[12] J. Sakellariou, K. Petsounis, S. Fassois, Vibration analysis based on-board fault detection in railway vehicle suspensions: a feasibility study, in: Proceedings of First National Conference on Recent Advances in Mechanical Engineering, Patras, Greece, 2001.
[13] S. Liberatore, G. Carman, Power spectral density analysis for damage identification and location, Journal of Sound and Vibration 274 (3–5) (2004) 761–776.
[14] D. Rizos, S. Fassois, Z. Marioli-Riga, A. Karanika, Vibration-based skin damage statistical detection and restoration assessment in a stiffened aircraft panel, Mechanical Systems and Signal Processing 22 (2008) 315–337.
[15] H. Hwang, C. Kim, Damage detection in structures using a few frequency response measurements, Journal of Sound and Vibration 270 (2004) 1–14.
[16] L. Ljung, System Identification: Theory for the User, second ed., Prentice-Hall, Upper Saddle River, NJ, 1999.
[17] H. Sohn, C. Farrar, N. Hunter, K. Worden, Structural health monitoring using statistical pattern recognition techniques, Journal of Dynamic Systems, Measurement, and Control 123 (4) (2001) 706–711.
[18] H. Sohn, D. Allen, K. Worden, C. Farrar, Statistical damage classification using sequential probability ratio tests, Structural Health Monitoring 2 (1) (2003) 57–74.
[19] H. Sohn, C. Farrar, Damage diagnosis using time series analysis of vibration signals, Smart Materials and Structures 10 (2001) 446–451.
[20] D. Adams, C. Farrar, Classifying linear and nonlinear structural damage using frequency domain arx models, Structural Health Monitoring 1 (2) (2002) 185–201.
[21] K. Nair, A. Kiremidjian, K. Law, Time series-based damage detection and localization algorithm with application to the asce benchmark structure, Journal of Sound and Vibration 291 (2006) 349–368.
[22] K. Nair, A. Kiremidjian, Time series based structural damage detection algorithm using gaussian mixtures modeling, Journal of Dynamic Systems, Measurement, and Control 129 (2007) 285–293.
[23] E. Carden, J. Brownjohn, Arma modelled time-series classification for structural health monitoring of civil infrastructure, Mechanical Systems and Signal Processing 22 (2) (2008) 295–314.
[24] M. Fugate, H. Sohn, C. Farrar, Vibration-based damage detection using statistical process control, Mechanical Systems and Signal Processing 15 (4) (2001) 103–119.
[25] S. Mattson, S. Pandit, Statistical moments of autoregressive model residuals for damage localization, Mechanical Systems and Signal Processing 20 (2006) 627–645.
[26] F. Gao, Y. Lu, An acceleration residual generation approach for structural damage identification, Journal of Sound and Vibration 319 (2009) 163–181.
[27] H. Zheng, A. Mita, Two-stage damage diagnosis based on the distance between arma models and pre-whitening filters, Smart Materials and Structures 16 (2007) 1829–1836.
[28] J. Sakellariou, S. Fassois, Stochastic output error vibration-based damage detection and assessment in structures under earthquake excitation, Journal of Sound and Vibration 297 (2006) 1048–1067.
[29] S. Fassois, Parametric identification of vibrating structures, in: S. Braun, D. Ewins, S. Rao (Eds.), Encyclopedia of Vibration, Academic Press, London, UK, 2001, pp. 673–685.
[30] S. Kay, Modern Spectral Estimation: Theory and Application, Prentice-Hall, New Jersey, 1988.
[31] J. Bendat, A. Piersol, Random Data: Analysis and Measurement Procedures, third ed., Wiley-Interscience, New York, 2000.
[32] J. Gertler, Fault Detection and Diagnosis in Engineering Systems, Marcel Dekker, New York, 1998.
[33] G. Box, G. Jenkins, G. Reinsel, Time Series Analysis: Forecasting and Control, third ed., Prentice-Hall, Englewood Cliffs, NJ, 1994.
[34] J. Hios, S. Fassois, Stochastic identification of temperature effects on the dynamics of a smart composite beam: assessment of multi-model and global model approaches, Smart Materials and Structures 18 (2009) 035011 (15pp.).
[35] P. Michaelides, S. Fassois, Stochastic identification of structural dynamics from multiple experiments—experimental variability analysis, in: Proceedings of the ISMA Conference on Noise and Vibration Engineering, Leuven, Belgium, 2008.
[36] J. Hios, S. Fassois, Statistical damage detection in a smart structure under different temperatures via vibration testing: a global model based approach, Smart Materials and Structures 413–414 (2009) 261–268.